Centrifuge Testing - Cyclic Loading of Suction Bucket Foundations in Undrained Sand

Technical Report | United States of America

04.72190024 2 | 11 September 2020
Final

Bureau of Ocean Energy Management (BOEM)

Document Control

Document Information

Project Title	Cyclic Loading of Suction Bucket Foundations in Undrained Sand
Document Title	Centrifuge Testing - Cyclic Loading of Suction Bucket Foundations in Undrained Sand
Fugro Project No.	824-003-00104.7219002404.72190024
Fugro Document No.	04.72190024
Issue Number	2
Issue Status	Final
Fugro Legal Entity	Fugro USA Land, Inc.
Issuing Office Address	1777 Botelho Drive, Suite 262, Walnut Creek, CA 94596

Client Information

Client	Bureau of Ocean Energy Management (BOEM)
Client Address	45600 Woodland Road, VAE-AMD, Sterling VA 20166-9216
Client Contact	Daniel P. O'Connell
Client Document No.	[Client Document No.]

Revision History

Issue	Date	Status	Comments on Content	Prepared By	Checked By	Approved By
1	August 14, 2020	For Review	Awaiting client comments	HEL/JZ	CE/PW	MM
2	September 11, 2020	Final		HEL/JZ	CE/PW	MM

Project Team

Initials	Name	Role
HEL	Han Eng Low	Project Team Lead
JZ	Julia (Fangyuan) Zhu	Project Engineer
CE	Carl Erbrich	Technical Authority
PW	Phil Watson	Technical Consultant
MM	Mohamed Mekkawy	Project Manager

FUGRO
Fugro USA Land, Inc.
1777 Botelho Drive
Suite 262
Walnut Creek, California 94596

Bureau of Ocean Energy Management (BOEM)/ Daniel P. O'Connell
45600 Woodland Road
VAE-AMD
Sterling VA 20166-9216

11 September 2020

Dear Mr. O'Connell,

Fugro USA Land, Inc. (Fugro) is pleased to present this draft report documenting our centrifuge and laboratory test results for cyclic loading of suction bucket foundations in undrained sands. This work was performed under the Bureau of Ocean Energy Management (MOEM) Technology Advancement Program (TAP), Contract No.140M0119C0002 dated March 22, 2019. The objective of this project is to improve methods of designing suction bucket foundations in sandy soil under long term cyclic loads. This report builds on knowledge gained from a previous numerical study, also performed by Fugro for BOEM, on the feasibility assessment of suction bucket foundations. To achieve the project objectives Fugro performed multi-bucket and mono-bucket centrifuge tests under various load sequence and frequency conditions. The centrifuge testing was performed at the University of Western Australia. The centrifuge tests were supplemented by a detailed laboratory classification, static and dynamic tests to ensure soil properties are fully documented and understood, and that the results are interpreted within the selected soil and boundary conditions. Further, based on the findings, the project team has provided recommendations for future research work in order to continue advancing suction bucket design.

We thank you for the opportunity to work on this project and we look forward to continuing our services in the future.

Yours faithfully,

Han Eng Low, Ph.D.
Principal Geotechnical Engineer & PSI Lead

Phil Watson, Ph.D.
Shell Professor of Offshore Engineering

Mohamed Mekkawy, Ph.D., P.E.
Northern California Manager

Thaleia Travasarou, Ph.D., G.E.
Manager Geoconsulting Americas

Executive Summary

This project was generated to provide high quality experimental model test data for offshore soil conditions relevant to the U.S. East Coast., to inform the design of suction bucket foundations in sandy soil subject to cyclic loading.

A comprehensive centrifuge testing program funded by the Bureau of Ocean Energy Management (BOEM) and administered by the U.S. Department of the Interior (DOI) Bureau of Safety and Environmental Enforcement (BSEE) has been conducted. This testing project was managed and conducted by Fugro Australia Marine (FAM) and Fugro USA Land (FUSALI), in collaboration with the University of Western Australia (UWA). Testing focused on collecting data on the response of suction buckets in dense to very dense sand under cyclic loading, including into tension, to inform upcoming offshore wind farm developments off the US East Coast. The program comprised a large number of centrifuge tests (23 multi-bucket tests and 8 mono-bucket tests across 9 individual samples), along with soil element tests on sand samples representative of the centrifuge samples. It is anticipated that the obtained data will facilitate the future development and calibration of design methodology for the design of suction buckets to support offshore wind turbines in dense to very dense sand.

Key advantages with the current dataset as compared to existing datasets available in the public domain are:

1. The cyclic load patterns that were adopted in the centrifuge tests are more realistic, attempting to mimic the random nature of storm loading. The majority of the published experimental studies on suction buckets feature packets of uniform or ordered cyclic loading.
2. Water cavitation was recognized as a critical issue in controlling the uplift response and hence much larger (and more realistic) water depths were modelled for these tests than in other public domain datasets.
3. The centrifuge tests were supplemented by a series of companion soil element tests that characterized the behavior of the tested sand. This is expected to facilitate back analysis and numerical simulation as part of future (and broader) research.
4. The dataset will allow direct comparison between the performance and efficiency of mono- and multi-bucket foundation configurations in the same soil.

Centrifuge test data collected for this project indicates that in dense to very dense sand a multi-bucket foundation system is a substantially more efficient foundation system than a mono-bucket system for resisting the high overturning moment loading associated with offshore wind turbines. This is because the “push-pull” loads between the windward bucket and leeward bucket of the multi-bucket system are much more efficiently resisted in the soil compared to the rotational failure mechanism that must be generated to support the mono-bucket system.

In addition, the test data also showed that, under favorable drainage conditions and with a sufficiently high cavitation pressure limit, the suction buckets of a multi-bucket foundation system can sustain two-way cyclic loading with significant cyclic tension loads mobilized on the windward bucket at close to zero average stress, with minimal permanent displacement. This could eliminate any perceived

requirement for expensive foundation ballast to offset the applied cyclic tension loads. It is anticipated that with further research using the data collected for this project, the 'multi-bucket' foundation system will be proven to be a technically viable (and hopefully economical) foundation option to support offshore wind turbines located offshore the USA in sea-beds comprised of dense to very dense sand.

Based on these observations, Section 6.2 summarizes recommendations for future work to allow the development of an improved design methodology to allow the design of cost-effective "multi-bucket" foundation systems for offshore wind turbines in dense to very dense sand.

This final report has been reviewed by the BSEE and approved for publication. Approval does not signify that the contents necessarily reflect the views and policies of the BSEE, nor does mention of the trade names or commercial products constitute endorsement or recommendation of use

Contents

Appendices

Figures in the Main Text

Tables in the Main Text

Abbreviations

BAA	Broad Agency Announcement
BOEM	Bureau of Ocean Energy Management
BSEE	Bureau of Safety and Environmental Enforcement
CADC	Anisotropically consolidated drained triaxial compression
CADE	Anisotropically consolidated drained triaxial extension
CAUC	Anisotropically consolidated undrained triaxial compression
CAUE	Anisotropically consolidated undrained triaxial extension
COFS	Centre for Offshore Foundation Systems
CPT	Cone penetrometer test
cSt	Centistokes
D	Diameter
DC	Direct Current
DigiDAQ	Data Acquisition System
DOI	Department of the Interior
D_r	Relative Density
EPPT	Excess Pore Pressure Transducers
FAM	Fugro Australia Marine Pty Ltd
Fugro agLAB	Fugro soil laboratory
FUSALI	Fugro USA Land, Inc.
g	Gram
G_0	Small strain shear modulus
Hz	Hertz
ISFOG	International Symposium on Frontier in Offshore Geotechnics
kg	Kilogram
kN/m^3	Kilonewton per meter cube
kPa	Kilopascal
L	Skirt Length
LDT	Linear Displacement Transducer
m	Meter
m/s	Meter per second

MHz	Megahertz
mm	Minimeter
mm/s	Minimeter per second
mm^3/s	Minimeter cube per second
NGCF	National Geotechnical Centrifuge Facility
OWT	Offshore Wind Turbine
PACS	Package Actuator Control System
PCPT	Piezocone Penetration Test
PP	Pore pressure
PPT	Pore Pressure Transducer
PSD	Particle Size Distribution
q_t	Cone Tip Resistance
rpm	Round per minute
R_a	Surface Roughness
t	Skirt Thickness
TP	Total Pressure
TPT	Total Pressure Transducer
US	United States
UWA	University of Western Australia
V/A	Vertical load divided by plan area of the model bucket
WEA	Wind Energy Area
z/L	Bucket vertical displacement (z) normalized with bucket skirt length (L)
Δz	Change in vertical displacement from the start of the cyclic load packet

1. Introduction

1.1 Background

Suction buckets have been used for over 20 years as a foundation option for offshore oil and gas facilities (Bye et. al., 1995; Tjelta, 2015). Depending on the water depth, soil conditions, and characteristics of the supported superstructure, mono-bucket or multi-bucket foundation systems can be designed to provide sufficient static and dynamic capacity and resist all design loads. As illustrated in Figure 1.1a, an offshore wind turbine (OWT) supported on a mono-bucket foundation systems relies on the moment capacity of the individual bucket foundation, which may put the windward edge of the bucket into net tension. For multi-bucket foundation systems, the overturning effect of wind and current acting on the OWT is principally resisted by "push-pull" effects between the windward bucket, where the vertical load (V_1 in Figure 1.1b) decreases, and the leeward bucket, where the vertical load (V_2 in Figure 1.1b) increases. In this case, the decreasing vertical load on the windward foundation that can put the entire foundation into net tension and is expected to be critical for design in sandy soils.

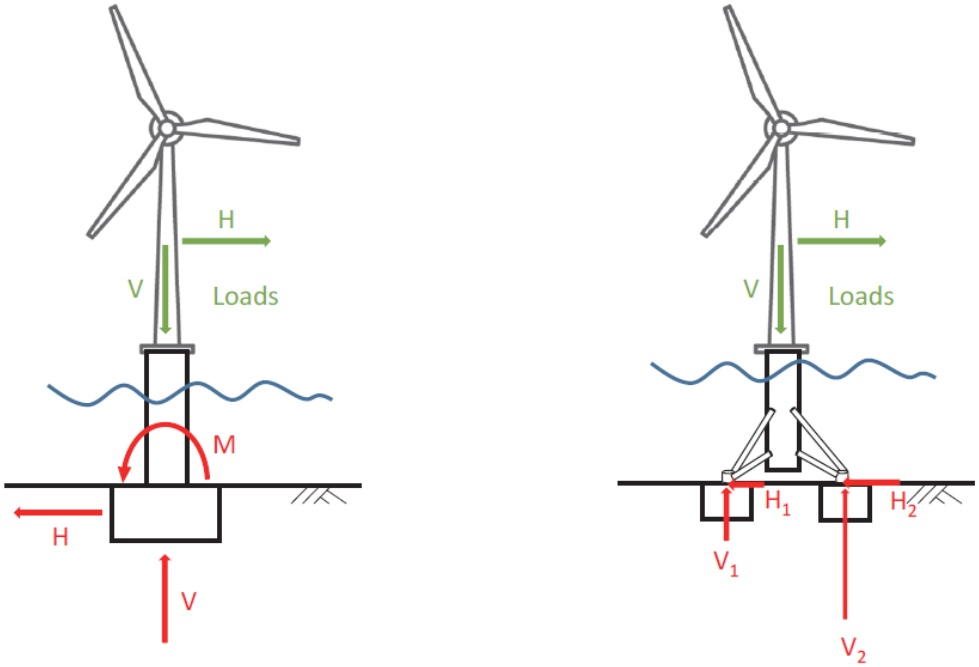

Figure 1.1: Simplified Loading Mechanisms for a) Mono-Bucket and b) Multi-Buckets in a Tripod Structure

OWTs have been operational in the European sector for over a decade but are relatively new in the U.S. These structures are particularly sensitive to dynamic loading conditions due to the combination of a relatively light weight structure and a wide range of cyclic loads. In addition, tight tolerances on permanent foundation movement are generally prescribed over

the OWT design life, in particular with respect to the allowable maximum tilt (typically limited to less than 0.5°).

As identified in a previous BSEE study (Fugro, 2016), the amount of suction bucket model test data available in the public domain is limited. The 2016 study also indicated that drainage conditions are an important aspect affecting the cyclic response of suction bucket foundations in cohesionless soils. Accordingly, there is a need for further model testing to fill the existed data gap and increase industry understanding of how these foundations behave under cyclic loading.

1.2 Project Description

Bureau of Ocean Energy Management (BOEM) awarded Contract No. 140M0119C0002 to Fugro USA Land, Inc. (FUSALI) for the project titled "Cyclic Loading of Suction Bucket Foundations in Undrained Sand". This project was proposed in response to Broad Agency Announcement (BAA number: E17PS00128) Topic 2 and is part of the Proposed Safety and Technology Verification Research Projects: Wind Power Structure Research.

Fugro Australia Marine Pty Ltd (FAM) collaborated with Fugro USA Land, Inc. (FUSALI) to coordinate the centrifuge model testing, subsequently performed at The University of Western Australia (UWA), and to perform soil element testing. FAM also led the data interpretation and reporting scope, in accordance with the proposal approved by BOEM. The ultimate objective of this project was to generate high quality and well documented experimental data for soil conditions relevant to U.S. offshore wind farms, in order to inform methods of designing suction bucket foundations in sandy soil under cyclic (primarily tension) loads.

1.3 Scope of Work

Completed scope of work for this project included:

- **Task 1 – Centrifuge Model Testing**. Multi-bucket and mono-bucket centrifuge tests were conducted at the National Geotechnical Centrifuge Facility (NGCF) at the Centre for Offshore Foundation Systems (COFS), UWA. Completed tasks include:
  a. Preparation of a detailed testing program with the primary focus of providing experimental data on mono- and multi-suction bucket foundation response under cyclic loading in soil with conditions similar to those at future and currently proposed US offshore wind farm sites.
  b. Provision of support and supervision during centrifuge testing to ensure the centrifuge tests were conducted according to the agreed plan and quality.
- **Task 2 – Laboratory Soil Element Testing**. Soil element tests were conducted at the Fugro's state-of-the-art geotechnical laboratory (Fugro agLAB) in Perth, Australia. Completed tasks include:
  a. Preparation of a detailed testing program to characterize the soil samples used in centrifuge testing.

b. Preparation of a representative soil samples, and performance of the planned soil element tests.
c. Provision of support and supervision during laboratory testing to ensure the soil element tests were conducted according to the agreed plan and quality.

- **Task 3 – Interpretation of the Test Results and Creation of Database**. Test results from centrifuge and soil element testing are interpreted and compiled into a database. This database is provided electronically in Excel format together with this report.
- **Task 4 – Recommendations for Future Research**. Based on observations from the centrifuge testing, key factors that affect suction bucket foundation response during cyclic loading in dense to very dense sand, and the performance and efficiency of mono- and multi-buckets as foundations for OWTs in dense to very dense sand were explored. Recommendations for future research required to develop guidelines for the design of efficient suction bucket foundations in dense to very dense sand were identified.
- **Task 5 – Project Management, Meetings and Teleconferences.** Communication via email and teleconference between Fugro and BOEM. Fugro also provided meeting minutes and progress reports documenting the project progress, status of technical requests, cost/budget, future planned work and other topics raised during meetings.
- **Task 6 – Reporting**. Raw and interpreted test data, discussion and recommendations are documented in this report. A conference paper titled "Cyclic Loading of Offshore Wind Turbine Suction Bucket Foundations in Sand: the Importance of Loading Frequency" has been prepared based on the results of the multi-bucket centrifuge tests conducted for this project. The paper has been accepted for publication at the 4th International Symposium on Frontier in Offshore Geotechnics (ISFOG 2020). Other publications are under consideration but considered out of scope.

1.4 Scope of Report

Following this introductory section, Section 2 presents an overview of the in-place response of suction bucket foundations in sand, the use of such foundations for offshore wind turbines, and the limitations of existing model testing available in the public domain. Section 3 presents details of the centrifuge model tests (multi-bucket and mono-bucket tests) conducted for this project, and provides an overview of the data acquired, while Section 4 discusses on the results themselves. Section 5 presents the soil element tests conducted for this project. Finally, Section 6 concludes the study and provides recommendations for future research.

1.5 Use of Report

This Report and its contents have been prepared for the purposes set out in the agreed scope of work, which forms part of the contract between Fugro and Bureau of Ocean Energy Management (BOEM) in relation to the design of suction bucket foundations in sandy soil subject to cyclic loading. This Report and its contents are provided solely for the use of Bureau of Ocean Energy Management (BOEM) for the agreed purpose and are not to be used or relied on outside of that purpose. This Report is to be read and used in its entirety and in

the context of the methodology, procedures and techniques used, and the circumstances and constraints under which the report was written. Sections or parts of the Report should not be read or relied upon out of context.

This technical work has been conducted, and this Report prepared, based on the assumptions identified in the Report and, where indicated in the Report, on information and data supplied by others. Fugro accepts no liability for any omission or inaccuracy in the information or data supplied by Bureau of Ocean Energy Management (BOEM) or its agents.

2. Literature Review

2.1 Overview of in-Place Response of Suction Bucket Foundations in Sand

The capacity and stiffness of suction buckets subject to static and cyclic load is affected by soil strength-increasing effects from consolidation and soil strength-decreasing effects from cyclic degradation. These competing effects are in turn affected by loading and soil conditions.

For sandy soils, consolidation times are expected to be short and full consolidation likely occurs under static loads. However, environmental load from wind gusts and waves are often sufficiently rapid to result in a partially drained to fully undrained response during individual load cycles. Over the duration of a 'storm' event, and reflecting fast drainage conditions, peak pore pressure accumulation may be modest.

Early examples where bucket foundations were adopted to support jacket structures in very dense sandy soils (Draupner E and Sleipner SLT structures; Bye et. al., 1995) were relatively heavy, with the buckets only subject to occasional cyclic tensile load under extreme events. Model testing was conducted to support these projects, as well as offshore field tests where both monotonic and cyclic tension loads were applied (Tjelta, 2015). These tests demonstrated that where the foundation load remained in compression, the resulting behavior was well understood. However, when the foundations were cycled into tension (from an average compression load) complex behaviors developed that required more detailed consideration.

Where cyclic loads were applied rapidly relative to consolidation times, excess pore pressures accumulated such that the foundation would undergo progressive downward settlement and/or tilting (i.e. cyclic undrained failure or "liquefaction" failure). It is important to note that regardless of whether the loads cycled from compression into tension, the net foundation movement was always downwards due to the average compression load. It was found that such failure mechanisms could be readily predicted through conventional methods widely used in the offshore foundation design industry.

When fully undrained (i.e. short term) uplift occurred, it was found that suction bucket foundations in dense sand could mobilize high uplift capacity as a result of passive suctions; and these suctions could be sustained for a period due to the strong tendency of such soils to dilate when sheared. However, under sustained tensile loading these foundations would inevitably pull-out under much lower loads, with the long-term capacities ultimately attributed to skin friction alone.

From these model test programs, it was identified that a "sweet spot" exists where the maximum tensile capacity of a suction bucket can be mobilized. This coincides with individual tensile load cycles being applied undrained, but where consolidation between individual load cycles was sufficiently fast to ensure there were no (or negligible) detrimental effects arising

from pore pressure accumulation (degrading undrained strength/ stiffness). As noted in Tjelta (2015) bucket foundations in sand may sit near to this "sweet spot", but to ensure a safe design, consideration needs to be given to scenarios where there is both more and less drainage than is desired for the optimum capacity.

2.2 Suction Bucket Foundations in Sand for Offshore Wind Turbines

Unlike the early oil and gas facilities, an OWT is a much lighter structure that is subject to high overturning moments. Inevitably, such structures will impose significant cyclic tensile stresses in the soil under certain design conditions. In addition, due to the relatively greater magnitude of the wind loads compared to wave loads, it is Fugro's experience that there may be periods where a net static tension load is applied simultaneously with a significant cyclic tension. In this context "tension" refers to the development of localized tensile stress at the bucket tip, and applies to both the windward edge of a mono-bucket foundation under predominately moment loading, and the windward leg(s) of a multi-bucket system under predominately vertical push-pull loading (i.e. V_1 in Figure 1.1b can be in tension).

From a multi-bucket foundation design perspective, loading conditions involving a small sustained tension overlaid with load cycles comprising much larger tensile stresses may be expected to lead to foundation "failure" that is characterized by progressive upward ratcheting movement which leads to system rotation. For a mono-bucket foundation, equally detrimental loading conditions may lead to progressive rotational movement of the entire foundation. In either case, this may lead to permanent tilt of the OWT, and the exceedance of strict design tolerances. The rate of progress of this movement is dependent on the foundation consolidation time relative to the applied loading. While this is a crucial design aspect for bucket foundation based OWTs in sand, there is currently minimal testing addressing this failure mechanism.

On some occasions cyclic tension loads have been mitigated by including ballast to partially offset the tension loads. For OWT foundations the cost of such a mitigation solution is likely to be high, thereby negating the economics of bucket foundations as a foundation solution. Accordingly, this project was conducted to explore the potential benefits of (i) high undrained tension capacity during transient tension loading; and (ii) pore water dissipation between large load cycles that eliminates potential degradation of the undrained strength and stiffness that would otherwise be caused by pore pressure accumulation induced as a result of the applied cyclic loading. The ultimate objective was therefore to provide data that would allow improved design practice and to assist with sustainable development of the offshore wind industry in the U.S.

Noting that in U.S. waters where wind farms are currently proposed, suction bucket foundations will (at least initially) most likely be installed in dense to very dense sands (Fugro, 2016), the focus of the model testing conducted in this project was to assess the response of suction bucket foundations in such soils.

2.3 Limitation of Existing Suction Bucket Model Test Database in the Public Domain

A comprehensive review of (public domain) model testing to explore the cyclic loading response of suction bucket foundation in sand is presented in Fugro (2016). In general, the limitations of the published model tests are:

- Some testing programs were performed in dry sands, or in samples that do not model representative drainage conditions occurring during individual load cycles (i.e. partially drained to undrained).
- Few tests have been performed with realistic storm loading sequences. The majority of the published model tests (e.g. Kelly et al., 2006; Bienen et al., 2018) are typically conducted using uniform cyclic loading regimes, or overly simplistic (ordered) storm load histories, which may not capture the potential benefit of pore water pressure dissipation between individual peak tensile loads. This is likely to be overly onerous for foundation design, leading to unnecessarily expensive foundations and potential invalidating the bucket foundation concept.
- Recent published experimental studies (e.g. Bienen et al., 2018) were conducted with low water depth. Obtained results were greatly affected by the cavitation pressure limit of the pore fluid used in the model tests and could lead to misconception that incorrectly invalidate the bucket foundation concept for OWTs.
- There is an absence of companion soil element test data, needed to characterize the soil behavior at the element level. This is critical as site-specific design methods use measured soil element behavior (such as monotonic and cyclic strength, coefficient of consolidation, compressibility etc.) to assess the performance of a foundation, and thereby select an appropriate foundation size. Without such information, model test data may lead to anecdotal findings, which cannot be used directly for back-analysis or numerical model calibration.
- There are no direct (like for like) comparisons of mono- and multi-bucket foundations for OWTs in the same soil.

In view of the above, a series of centrifuge tests (appropriately supported by soil element tests) were carried out in this project to investigate: (i) the effect of drainage conditions (i.e., pore pressure generation and dissipation) during transient and realistic cyclic loading of suction buckets; and (ii) differences between mono- and multi-bucket foundations.

3. Centrifuge Model Testing

Centrifuge tests presented in this report were conducted at the National Geotechnical Centrifuge Facility (NGCF) at The University of Western Australia using a 1.8 m radius beam centrifuge (Randolph et al. 1991). Tests were conducted at a nominal acceleration of 100 g (applied at half the skirt depth).

Centrifuge modelling involves increasing the acceleration such that stresses in the model are identical with the prototype. As the behavior of the sand used in the current project is stress dependent, matching the stress will ensures the soil response observed in the model is representative of the soil response observed in the prototype.

This section provides details of the testing facilities, instrumentation, soil samples, testing program and results for multi- and mono-bucket centrifuge testing.

3.1 Testing Facilities

3.1.1 UWA Beam Centrifuge

The National Geotechnical Centrifuge Facility (NGCF) at The University of Western Australia (UWA) currently operates three geotechnical centrifuges, undertaking a wide range of specialist testing for research and industry purposes.

The centrifuge used in this project was commissioned in 1989 and is an Acutronic Model 661 geotechnical centrifuge. It has a swinging platform radius of 1.8 m and is rated at 40 g-tons – which equates to a maximum payload of 200 kg at a maximum operating acceleration of 200 g. At the maximum acceleration of 200 g the rotational speed is 340 rpm, with a platform velocity of 63.9 m/s. The platform supports standard rectangular ‘strongboxes’ which have plan dimensions of 650 × 390 mm and are 325 mm deep, representing (at 100 g) a field scale test bed of up to 65 m long by 39 m wide. For this project, the height of the strongboxes was extended to 425 mm to allow additional free fluid height for the suction bucket testing. A complete description of the beam centrifuge is provided by Randolph et al. (1991).

Headroom above the strongbox allows equipment to be mounted to perform ‘inflight’ events, such as robotic manipulation of a model foundation. The whole machine is housed in a specially constructed circular reinforced concrete chamber that is air-conditioned to maintain a constant temperature during long tests and to avoid seasonal variations. The beam centrifuge is shown on Plate 1.

3.1.2 Robotic Control

Tests described in this report involved the manipulation of a model suction bucket and a miniature piezocone penetrometer using a dual axis electrical actuator, and the in-flight suction installation of a model suction bucket using a syringe pump.

The actuator was mounted on top of strongbox (as shown in Plate 1), in which the soil sample was contained, and allows vertical and horizontal movements (and loads) to be imposed on the suction bucket and/or penetrometer. Motion is provided by two DC servomotors that drive vertical and horizontal leadscrews. The actuator used in these tests has a vertical travel of up to 240 mm and a horizontal travel of 185 mm, which can be achieved at variable speeds up to approximately 3 mm/s.

The syringe pump was mounted to the side of the strongbox and was connected to the top of the model suction bucket via a plastic pipe and a 3-way valve (as shown on Plate 2 and Plate 3). The syringe pump was specially designed to apply suction inside model suction buckets in a high gravity field, to allow suction installation without stopping the centrifuge (House, 2002).

The 3-way valve was manipulated in-flight using a motor and wire arrangement (as shown on Plate 2 and Plate 3) to allow (i) venting of the model suction bucket during self-weight installation; (ii) hydraulic connection of the model suction bucket to the syringe pump during suction installation; and (iii) sealing of the model suction bucket during the load test.

The actuator, syringe pump and 3-way valve are all controlled using the UWA actuation control system, PACS (Package Actuator Control System, Catania et al. (2010)). The primary control software runs on a computer mounted on the centrifuge, acting as a slave to a master computer in the centrifuge control room, with communication between the two via an Ethernet link across an optical slip ring. Load or displacement-controlled operation can be achieved using feedback loops, which may limit the quality of the load control under high displacement velocities.

3.1.3 Data Acquisition

Data were acquired using a novel high-speed data acquisition system (DigiDAQ) developed at UWA for centrifuge testing (Gaudin et al., 2009). The DigiDAQ system consists of up to 8 separate miniature units mounted on the centrifuge basket, communicating with the control room via Ethernet. Each unit is capable of powering and monitoring 8 instrument channels at a sampling rate of up to 1 MHz at 16-bit resolution. Data obtained during testing is stored through on-board solid state memory and may also be streamed in real-time at low frequency (typically 10 Hz) – this was used during the testing.

Unlike PC-based data acquisition solutions, this system performs the full sequence of amplification, conditioning, digitization and storage on a single circuit board via an independent micro-controller allocated to each pair of instrumented channels. This arrangement is efficient, compact and physically robust, to suit the centrifuge environment.

A specific LabVIEW user interface permits control and monitoring of each box, including adjustment of the sampling rate, the trigger mode and the live display of the measured quantities.

3.2 Model Bucket and Test Setup

3.2.1 Multi-bucket Test

The model used for multi-bucket centrifuge testing was made of aluminum. It has a diameter (D) of 80 mm, skirt length (L) of 40 mm and skirt thickness (t) of 0.5 mm – which at 100g corresponds to a prototype suction bucket with D = 8 m, L = 4 m and t = 50 mm. The surface of the skirt is smooth, with surface roughness R_a ranging from 0.6 to 1 µm, as measured with a roughness profilometer.

The model bucket was instrumented with a pore pressure transducer (PPT) and total pressure transducer (TPT) at the bucket lid invert to measure changes in pore pressure and contact pressure. A second TPT was installed on the top of the bucket lid to measure the hydrostatic pore pressure and thus allow determination of excess pore pressure inside the bucket. A load cell was used to measure the applied vertical load, and a linear displacement transducer (LDT) was used to measure vertical displacement during testing. Photos of the model bucket and setup are shown on Plate 2.

The model bucket was manipulated using the dual axis (vertical and horizontal) electrical actuator that is described in Section 3.1.2. The vertical axis of the actuator was used in testing to install the bucket during self-weight penetration, maintain a constant vertical load on the bucket during suction installation and apply pure vertical monotonic/cyclic load to simulate loading conditions on a windward bucket of a multi-bucket foundation system.

Suction installation of the suction bucket was achieved using the syringe pump described above, which extracts fluid from inside the caisson, creating differential pressure across the bucket lid – leading to penetration of the bucket, with the 'self-weight' maintained constant.

3.2.2 Mono-bucket Test

The model suction bucket used for mono-bucket centrifuge testing was also made of aluminum. It has a diameter (D) of 140 mm, skirt length (L) of 70 mm and skirt thickness (t) of 0.5 mm – which at 100g corresponds to a prototype suction bucket with D = 14 m, L = 7 m and t = 80 mm. The skirt has similar surface roughness to the multi-bucket model. It should be noted that the model dimensions were selected to have the same plan and skirt area as three buckets for the multi-bucket model – with the intention that this would facilitate a rough comparison of efficiency between the multi-bucket and mono-bucket foundation systems.

The model bucket was instrumented with two excess pore pressure transducers (EPPT) and three total pressure transducers (TPT) at the bucket lid invert (as shown on Plate 3) to measure changes in pore pressure and contact pressure. As shown on Plate 3, the sensors were installed diametrically across the bucket invert, and aligned with the direction of horizontal load during testing. In addition, similar to the model bucket used in the multi-bucket testing, a TPT was also installed on the top of the bucket lid to measure the hydrostatic pore pressure at top of the suction bucket.

A dual-axis load pin (mounted in ball bearings) was used to measure the applied vertical and horizontal loads during testing, while an additional high capacity load cell mounted in loading bracket was used to measure the vertical load in cases where the model required jacking-in to achieve full installation. Laser sensors were used to measure vertical displacement and rotation of the model bucket during testing. Photos of the model bucket and setup are shown on Plate 3.

3.3 Soil Samples

3.3.1 UWA Superfine Silica Sand

A review of the soil conditions for US East Coast offshore wind farm sites indicated that:

1. In the North Atlantic areas allocated to offshore wind (e.g. Massachusetts), as sites move further from shore and into deeper water, the top 10 m of the seabed often comprises fine to medium, relatively clean (low fines content) sand, with occasional interbedded thin clay/ silt layers;
2. In the mid-Atlantic areas allocated to offshore wind (e.g. the New Jersey and Virginia) the top 10 m of seabed often comprises silty/ clayey fine sand with interbedded clay layers.

Plate 4 illustrates the range of particle distribution for soils in the top 10 m of the seabed at one wind farm site offshore Massachusetts WEA, where seabed soil conditions may suit suction bucket foundations.

Sand selected for centrifuge testing is a fine to medium sub-angular silica sand (called UWA superfine silica sand) with basic soil properties is summarized in Table 3.1. As shown on Plate 4, the particle size distribution curve of this sand falls within the particle distribution range for the sandy soils at this site – making this representative of sandy soil sites encountered in the designated North Atlantic wind farm areas.

Table 3.1: Index Properties of UWA Super Fine Silica Sand (Chow et al., 2018)

Soil Properties	Silica Sand
Specific gravity, G_s	2.67(1)
Particle size, D_{10}, D_{50}, D_{60} (mm)	D_{10}=0.09; D_{50}=0.19; D_{60}=0.21(2)
Coefficient of uniformity, C_u	2.24(2)
Coefficient of curvature, C_c	1.13(2)
Minimum dry density, ρ_{min} (kg/m^3)	1497(1)
Maximum dry density, ρ_{max} (kg/m^3)	1774(1)
Note: (1): Reported in Chow et al. (2018) (2): Measured in this project.	

3.3.2 Sample Preparation

The soil samples for both multi- and mono-bucket centrifuge testing were prepared using the same approach.

First, the sand was placed in the strongbox via dry pluviation to achieve a consistent relative density (D_r) of approximately 80%. This relative density was selected to match commonly encountered offshore conditions. The estimated D_r for each sample, as determined from global measurements of soil mass and volume, is summarized in Table 3.2.

Table 3.2: Estimated Relative Density and Measured METHOCEL™ Viscosity for Each Soil Sample

Testing	Soil Sample No.	Relative Density (%)	METHOCEL™ Viscosity at 19°C (cSt)	
			In Container(1)	Above the Soil Sample(2)
Multi-bucket Testing	Sample 1	77	453	-
	Sample 2	81	465	-
	Sample 3	63(3)	464	-
	Sample 4	85	461	-
	Sample 5	90	465	-
Mono-bucket Testing	Sample 6	89	467 (370)	317
	Sample 7	89	467 (376)	190
	Sample 8	82	467 (381)	145
	Sample 9	87	488 (383)	341

Note:
(1): The measured viscosity for METHOCEL™ in container before it was used to saturate the soil samples. The viscosity values presented in brackets are the values measured on the METHOCEL™ remained in the container after the mono-bucket centrifuge testing was conducted approximately 2 months after the first measurement was taken).
(2): The measured viscosity for METHOCEL™ above the soil sample after saturation i.e. from testing done on the pore fluid that has passed through the soil sample. The reason for the reduction in viscosity is not currently known.
(3): The method used to calculate sample density was improved throughout the testing program, and the range in density reported for the initial samples (used for multi-bucket testing) is not thought to be realistic. The values reported for samples used for mono-bucket testing are believed more credible and thought to be representative of all samples (which were prepared the same way). This is consistent with the CPT results, which show good consistency across all soil samples (see Plate 6).

Soil samples were saturated from the sample base with cellulose ether (METHOCEL™). This pore fluid was adopted (instead of water with viscosity of 1 centistokes, cSt) in order to lower the effective permeability of the sand and allow testing to be conducted under a representative range of drainage conditions (from fully drained to nearly undrained conditions). Measured viscosity values for the METHOCEL™ in the container and above the sand sample for each sample are summarized in Table 3.2. It can be seen that there is some variability in viscosity, depending on where (and when) the sample was collected for testing. The reason for these discrepancies, especially when testing the fluid after sample saturation, is unclear.

After preparation, the soil sample was subjected to 5 ramp up/ramp down cycles to 100g to assist with sample saturation and to make minimize the effect of later ramp up/ramp up cycles between individual suction bucket tests.

Soil samples used in the multi-bucket testing and mono-bucket testing had heights of approximately 120 mm (prototype 12 m) and 150 mm (prototype 15 m), respectively. Free fluid height above the soil samples during the centrifuge testing was approximately 200 to

240 mm (prototype 20 to 24 m) for the multi-bucket testing and 180 to 190 mm (prototype 18 to 19 m) for the mono-bucket testing, respectively. In addition, some multi-bucket tests (as indicated in Table 3.2) were conducted with a reduced free fluid height of approximately 90 to 100 mm (prototype 9 to 10 m) to investigate the effect of water depth on the monotonic and cyclic pull-out responses (see details in Section 3.4).

3.3.3 Sample Characterization

Cone penetrometer tests (CPTs) were conducted in-flight in each centrifuge sample (for both multi- and mono-bucket testing) to provide a basis for comparing the strength consistency between the tested soil samples. In each centrifuge sample, the CPT tests were conducted both before and after the suction bucket testing.

CPTs were conducted using a miniature (model) cone penetrometer with diameter (d) of 5 mm at penetration rates (v) ranging from 0.01 to 5 mm/s (with the majority of the CPTs conducted at 0.5 mm/s). A small number of piezocone penetration tests (PCPTs) were also conducted in the samples used for the mono-bucket testing, using a piezocone with diameter of 10 mm and penetration rates ranging from 0.25 to 2.5 mm/s. All the CPTs and PCPTs were conducted at approximately the same location across the centrifuge samples and the indicative locations are shown on Plate 5.

Cone tip resistance (q_t) profiles measured in each sample are presented on Plate 6. Despite differences in penetration rate, are broadly consistent across all 9 samples. Exceptions are the post multi-bucket testing CPTs in Sample 4 (possibly due to disturbance from the sample being removed and tested later in the schedule) and the CPTs conducted near the side of the strongbox in Sample 6 and Sample 9 (possibly due to localized sample variability).

It can be noted on Plate 6 that at the same prototype depth, the q_t measured by the CPTs are generally higher than those measured by PCPTs, due to the difference in cone diameter.

3.4 Testing Program

3.4.1 Multi-bucket Test

The objectives of multi-bucket centrifuge testing were (broadly) to investigate the effects of excess pore pressure dissipation (i.e. drainage condition) and storm load sequence on a multi-bucket foundation installed in dense to very dense sand. A total of 23 multi-bucket centrifuge tests were performed, including:

- 6 monotonic pull-out tests;
- 11 random storm cyclic vertical load tests;
- 4 uniform cyclic vertical load tests; and
- 2 ordered storm cyclic vertical load tests.

In each test, the foundation was subjected to pure vertical load to simulate loading conditions at the windward leg of a multi-bucket foundation system under predominantly ‘push-pull’ loading – whereby the foundation can be loaded into tension, which may be

critical for design. After each cyclic vertical load test, a post-cyclic monotonic pull-out test was also performed to investigate the monotonic pull-out response after the bucket was subject to packets of cyclic vertical loading.

Table 3.3 summarizes the multi-bucket test program, in which the magnitude of compression/uplift is expressed as vertical stress (i.e. V/A where V is the vertical load and A is the plan area of the suction bucket). In each test, the Test ID indicates the test type, number and loading details. For example, M1_3 refers to the first monotonic pull-out test with vertical pull-out rate of 3 mm/s, whereas R60_160_0.1 refers to random ('R') storm cyclic loading about an average cyclic vertical stress of 60 kPa, with a maximum (first packet) cyclic vertical stress amplitude of 160 kPa, and a maximum cyclic load frequency of 0.1 Hz. In Table 3.3, Test IDs start with 'O' and 'U' are used to refer to tests with ordered storm and uniform cyclic loading respectively.

Note that the cyclic tests involved either one cyclic packet or three cyclic packets, which was to investigate the suction bucket cyclic vertical load response when its surrounding soil conditions were changed by previous cyclic load packet(s).

In summary, the testing program included:

- Tests to explore the monotonic pull-out response under undrained, partially drained and drained conditions – M2_3, M4_1, M5_0.15 and M6_0.001;
- Tests to investigate suction bucket responses under random storm cyclic loading for the targeted range of average vertical stress (i.e. 0 kPa and 60 kPa), cyclic vertical stress amplitude (100 kPa to 260 kPa) and cyclic load frequency (0.1 Hz to 1.8 Hz) – R60_160_0.1 to R60_260_1.8 and R0_100_0.1 to R0_200_0.6;
- Tests to investigate the number of 'equivalent cycles' of uniform cyclic loading that could results in response comparable to the response under random storm cyclic loading – U60_160_0.1, U60_160_0.6, U60_210_0.075 and U60_260_0.3;
- Tests to investigate the effect of cyclic load sequence (ordered vs random) on suction bucket responses – O60_260_0.6 and O0_200_0.6;
- Tests to investigate the effect of water depth (pore fluid cavitation limit) on suction bucket monotonic and cyclic load responses – M3_3(L), R60_260_0.6(L) and R0_200_0.6(L); and
- Tests to investigate the effect of installation method (jacked-in vs suction installation) on the suction bucket undrained pull-out response – M1_3(J).

3.4.2 Mono-bucket Test

The objectives of the mono-bucket centrifuge testing were (broadly) to investigate the effect of excess pore pressure dissipation (i.e. drainage condition) on mono-bucket foundation response, and to explore the differences between mono- and multi-bucket foundation response under random storm cyclic loading. A total of 8 mono-bucket centrifuge tests were performed, including:

- 3 monotonic 'push-over' tests; and
- 5 random storm cyclic load tests.

In each test, the mono-bucket was subjected to pure horizontal load at a height of 350 mm (prototype 35 m) above the soil surface (i.e. the eccentricity, e shown on Plate 7) to simulate loading of a mono-bucket foundation system for an OWTs. Following each cyclic test, a monotonic push-over test was also performed to investigate the response of the mono-bucket after it was subject to cyclic loading.

Table 3.4 summarizes the mono-bucket test program. The self-weight of the foundation is 120 kPa and remains constant throughout the tests, with the magnitude of horizontal load expressed in both model and prototype scale. In each test, the Test ID indicates the test type, number and loading detail. For example, M1_3 refers to the first monotonic push-over test with horizontal displacement rate of 3 mm/s, whereas R45_110_0.6 refers to the 'random' storm cyclic horizontal load test with an average cyclic horizontal load of 45 N, a maximum cyclic horizontal load amplitude of 110 N and a maximum cyclic load frequency of 0.6 Hz.

Note that all cyclic horizontal load tests involved three cyclic load packets to investigate the mono-bucket foundation responses when its surrounding soil conditions were changed by previous cyclic load packet(s).

In summary, the test program included:

- Tests to explore the monotonic push-over response under undrained and drained conditions – M1_3, M1_3r and M2_0.003; and
- Tests to investigate the mono-bucket foundation responses under random storm cyclic horizontal loading for a range of average cyclic horizontal load (45 N and 90 N), cyclic horizontal load amplitude (110 N to 220 N) and cyclic load frequency (0.6 Hz to 1.5 Hz) – R45_110_0.6, R45_110_0.6r, R90_110_0.6, R45_110_0.15 and R45_110_1.5.

3.5 Cyclic Load Sequence and Frequency

3.5.1 Multi-bucket Tests

For the multi-bucket tests, the cyclic vertical stress amplitude summarized in Table 3.3 corresponds to the maximum vertical stress applied within a cyclic load packet – which could be the same for different cyclic load sequences. Three type of cyclic load sequences were simulated in the multi-bucket tests i.e. random, uniform and ordered, which are discussed further below and presented on Plate 8 . Note that each individual load cycle was applied using a sinusoidal waveform.

The 'random' storm load sequence simulated in the multi-bucket tests were generated semi-randomly from the 6-hour duration peak storm load composition outlined in Andersen (1991) and summarized in Table 3.5. The sequence was generated by placing the largest cyclic stress amplitude at the middle of the load sequence. The next 60 largest cycles (i.e. those with amplitude equal to or greater than 70% of the maximum amplitude) were then

placed evenly at either side of the peak load cycle, at a constant time interval and in decreasing order toward both ends of the load sequence. This was intended to simulate the gradual ramp-up / ramp-down evident in real storms. The remaining (small) cycles were distributed randomly between the pre-arranged (large) cycles. Individual packets were then uniformly scaled according to the targeted maximum stress amplitude (see Table 3.3), leading to the generated 'random' storm load sequences presented on Plate 8a and Plate 8b.

Similar to the random storm load sequence, the ordered storm load sequences simulated in the multi-bucket tests were also generated based on the 6-hour duration peak storm load composition summarized in Table 3.5. In this case, the sequence was generated by placing the largest amplitude cycle at the middle of the load sequence, with the remaining cycles places in groups on either side of the largest amplitude cycle, as presented on Plate 8d. Individual packets were then uniformly scaled according to the targeted maximum stress amplitude, as summarized in Table 3.3.

The frequency for each load cycle within a random and ordered storm load sequences was determined according to the relationship between load frequency and cyclic stress amplitude, shown on Plate 9. These relationships were used to (roughly) simulate the increase in period for (extremely) large waves, while also improving load control in the centrifuge for cases where larger vertical displacement was expected. The frequency used to describe each load cycle in each test reflects the stress amplitude in the load cycle being described.

For the uniform cyclic load tests, the targeted cyclic frequency and amplitude were maintained constant throughout the cyclic load packet, as shown on Plate 8c.

3.5.2 Mono-bucket Tests

For the mono-bucket tests, the cyclic horizontal load amplitude summarized in Table 3.4 corresponds to the maximum horizontal load amplitude within a cyclic load packet. In the mono-bucket tests, only 'random' cyclic horizontal load sequence was simulated, and Plate 10 presents the variation of cyclic horizontal load amplitude with cycle number for all cyclic load packets simulated in the mono-bucket testing program.

Random storm sequences simulated in the mono-bucket tests were generated using the same procedure used to generate the random storm sequence for the multi-bucket tests. In contrast to the multi-bucket tests however, the frequency of individual load cycles in each mono-bucket test was maintained constant throughout the cyclic load packet.

3.6 Testing Procedure

3.6.1 Multi-bucket Test

In each multi-bucket test, a realistic installation process was simulated which involved the following testing procedure and is schematically shown on Plate 11:

- **Self-weight penetration**. To simulate self-weight penetration, the model bucket was pushed (vented) at a constant penetration rate of 0.1mm/s (model scale) to mimic a slow

set-down process that does not unduly disturb the sand bed. The simulated bucket self-weight was determined based on the assumption of a 700 tons (prototype) tripod jacket founded on three buckets, with each bucket having a self-weight of 120 tons (prototype). This equates to static (still water) vertical stress of 70 kPa on each bucket. When the vertical stress reached this level, the valve on the bucket lid was switched from vented condition to forming a hydraulic connection with the syringe pump to facilitate suction installation.

- **Suction installation**. Suction installation of the suction bucket was achieved by pumping the fluid from the interior of the bucket at a constant flow rate of 784 mm^3/s (model scale), whilst maintaining the vertical stress constant at 70 kPa. Installation was deemed complete when the suction pressure beneath bucket lid increased markedly, signifying contact of the bucket lid with the surface of the soil sample. In some tests, the bucket could not be fully installed using suction, possibly due to the entrapment of air bubbles in the syringe pump. In these tests, full installation of suction bucket was achieved by jacking the bucket (vented) at a constant penetration rate of 0.1 mm/s (model scale) until a sudden increase in resistance was observed. After full installation was achieved, the bucket was sealed by closing the valve on the bucket lid.
- **Application of additional self-weight**. In this step, the vertical stress was increased from 70 kPa to 120 kPa, in order to simulate the increase in self-weight due to the installation of the wind turbine above the jacket. Vertical load was increased in a single step and then held constant, allowing the dissipation of excess pore pressure generated by the instantaneous vertical load increase.
- **Pre-shearing**. Following the dissipation of excess pore pressure, a pre-shearing stage was conducted. In this pre-shearing stage, 400 cycles of small-amplitude cyclic vertical stress (± 6 kPa) were applied around the average stress of 120 kPa to the bucket. The objectives of this pre-shearing stage are to simulate small cyclic load events that may occur before a design storm, and to capture the 'bedding-in' process experienced in the field (Andersen, 2015). Following the pre-shearing stage, the vertical stress was held constant at 120 kPa to allow the dissipation of excess pore pressure generated during the pre-shearing stage.
- **Monotonic or cyclic loading**. Following the dissipation of excess pore pressure, vertical stress was decreased in a single step change to the average vertical stress targeted for each planned cyclic load packet (as summarized in Table 3.3). The reduction in stress simulates the reduction in vertical stress on the windward leg, due to the 'push-pull' effect caused by (assumed constant) wind and current loads acting on the turbine tower. Vertical stress was then held constant to allow the dissipation of excess pore pressure generated by the instantaneous vertical stress increase. For monotonic tests, the was then pulled-out at the target vertical pull-out rate summarized in Table 3.3. For cyclic vertical load tests, the bucket was then cyclically loaded under conditions of load control to achieve the targeted sequence of each cyclic load packet, as summarized in Table 3.3. Cycling was stopped when the accumulated vertical displacement exceeds 10% of the bucket diameter or at the end of the planned sequence, whichever came earlier. In tests

with three cyclic load packets, sufficient time was allowed between each packet to dissipate the generated excess pore pressure before the start of the subsequent cyclic load packet.

- **Post-cyclic monotonic loading**. At the end of each cyclic load test and after the excess pore pressure generated by the last cyclic load packet was dissipated, the model bucket was pulled out monotonically at the vertical displacement rate that was observed during the peak load cycle of the first cyclic load packet of the test, as summarized in Table 3.3.

3.6.2 Mono-bucket Test

Similar to the multi-bucket test, a realistic installation process was simulated in each mono-bucket test, following the testing procedure described below and shown schematically on Plate 12:

- **Self-weight penetration**. To simulate self-weight penetration, the model bucket was pushed (vented) at a constant penetration rate of 0.1mm/s (model scale) to mimic a slow set-down process that does not unduly disturb the sand bed. In this case, the simulated bucket self-weight was determined based on the assumption of a 700 tons tower founded on a mono-bucket foundation with a self-weight of 370 tons – equivalent to a vertical stress of approximately 70 kPa. When the vertical stress reached this level, the valve on the bucket lid was switched from the vented condition to forming a hydraulic connection with the syringe pump to facilitate suction installation.
- **Suction installation**. Suction installation of the suction bucket was achieved by pumping the fluid from the interior of the bucket at flow rates between 2,000 to 10,000 mm^3/s (model scale), whilst maintaining the vertical stress constant at 70 kPa. Installation was deemed complete when the suction pressure beneath bucket lid increased markedly, signifying contact of the bucket lid with the surface of the soil sample. In most of the tests, the model bucket could not be fully installed using suction – due either to the syringe pump reached its (volume) capacity or the entrapment of air bubbles in the syringe pump.
- **Application of additional self-weight**. In this step, the vertical stress was increased (with the bucket vented) from 70 kPa to 120 kPa to simulate the increase in self-weight due to installation of the wind turbine. Vertical stress was increased in a single step and then held constant, allowing the dissipation of excess pore pressure generated by the instantaneous stress increase. The 120 kPa was then held constant for the remainder of the test. Note that, where required to achieve full touchdown, the model bucket was first jacked-in (vented) at a constant penetration rate of 0.1 mm/s (model scale) to ensure full touchdown, before the vertical stress was maintained at 120 kPa and allowing dissipation. The bucket was then sealed by closing the valve on the bucket lid.
- **Pre-shearing**. Following the dissipation of excess pore pressure, a pre-shearing stage was conducted. In this stage, 400 cycles of small-amplitude cyclic horizontal load (± 5 N in all tests except tests M1_3 and M2_0.003, where ± 10 N was used) were applied around an average horizontal load (6 N for all tests with the exception of tests M1_3 and

M2_0.003, where 0 N was used). The objectives of the pre-shearing stage are to simulate small cyclic load events that may occur before a design storm and to capture the 'bedding-in' process experienced in the field (Andersen, 2015). Following the pre-shearing stage, the vertical stress was held constant at 120 kPa and horizontal load at 0 N to allow the dissipation of excess pore pressure generated during the pre-shearing stage.

- **Monotonic or cyclic loading**. For the monotonic push-over tests, the bucket was subjected to push-over at a height of 350 mm (prototype 35 m) above the soil surface, using the targeted horizontal displacement rate summarized in Table 3.4. For the cyclic horizontal load tests, the bucket was cyclically loaded at a comparable height, but using load-control to apply the targeted cyclic load packet summarized in Table 3.4. Cycling was stopped when the accumulated bucket rotation exceeded 3° or at the end of the planned cyclic load packet, wherever came earlier. In all the tests, sufficient time was allowed between the cyclic load packets to dissipate the generated excess pore pressure before the start of the subsequent cyclic load packet.
- **Post-cyclic monotonic loading**. At the end of each cyclic test and after the excess pore pressure generated by the last cyclic load packet was dissipated, the model bucket was pushed over monotonically (via load applied at the same height above the soil surface) and using the horizontal displacement rate observed during the peak load cycle of the first cyclic load packet of the test, as summarized in Table 3.4.

Table 3.3: Multi-Bucket Testing Program

No.	Test ID	Test Nature	Soil Sample	Load Frequency[3] (Hz)	Average Cyclic Vertical Stress (kPa)	Maximum Cyclic Vertical Stress Amplitude (kPa)			Number of Cycles			Displacement Rate for Monotonic Pull-out[4] (mm/s)
						Packet 1	Packet 2	Packet 3	Packet 1	Packet 2	Packet 3	
1A	M1_3(J)[2]	Monotonic	Sample 1	-	-	-	-	-	-	-	-	3
1B	M2_3	Monotonic	Sample 1	-	-	-	-	-	-	-	-	3
1C	M3_3(L)[1]	Monotonic	Sample 2	-	-	-	-	-	-	-	-	3
2	M4_1	Monotonic	Sample 2	-	-	-	-	-	-	-	-	1
3	M5_0.15	Monotonic	Sample 2	-	-	-	-	-	-	-	-	0.15
4	M6_0.001[5]	Monotonic	Sample 5	-	-	-	-	-	-	-	-	0.001
5	R60_160_0.1	Random Storm	Sample 2	0.1	60	160	210	160	1800	1800	1800	0.11
6	R60_160_0.6	Random Storm	Sample 1	0.6	60	160	260	160	1800	1800	1800	0.9
7	R60_210_0.1	Random Storm	Sample 2	0.075-0.1	60	210	-	-	1800	-	-	0.25
8A	R60_260_0.6	Random Storm	Sample 1	0.3-0.6	60	260	-	-	1800	-	-	1.1
8B	R60_260_0.6(L)[1]	Random Storm	Sample 4	0.3-0.6	60	260	-	-	1800	-	-	0.7
9	R60_260_1.8	Random Storm	Sample 5	0.9-1.8	60	260	-	-	1800	-	-	1.9
10	R0_100_0.1	Random Storm	Sample 3	0.1	0	100	150	100	1800	550	1800	0.1
11	R0_100_0.6	Random Storm	Sample 5	0.6	0	100	200	100	1800	1800	1800	0.15

No.	Test ID	Test Nature	Soil Sample	Load Frequency[3] (Hz)	Average Cyclic Vertical Stress (kPa)	Maximum Cyclic Vertical Stress Amplitude (kPa)			Number of Cycles			Displacement Rate for Monotonic Pull-out[4] (mm/s)
						Packet 1	Packet 2	Packet 3	Packet 1	Packet 2	Packet 3	
12	R0_150_0.1	Random Storm	Sample 3	0.1	0	150	-	-	950	-	-	0.4
13A	R0_200_0.6	Random Storm	Sample 3	0.48-0.6	0	200	-	-	1800	-	-	1
13B	R0_200_0.6(L)[1]	Random Storm	Sample 3	0.6	0	200	-	-	360	-	-	1.9
14	U60_160_0.1	Uniform Cyclic	Sample 4	0.1	60	160	210	160	360	270	360	0.08
15	U60_160_0.6	Uniform Cyclic	Sample 4	0.6	60	160	260	160	2160	1080	2160	0.5
16	U60_210_0.075	Uniform Cyclic	Sample 4	0.075	60	210	-	-	270	-	-	0.2
17	U60_260_0.3	Uniform Cyclic	Sample 4	0.3	60	260	-	-	550	-	-	0.16
18	O60_260_0.6	Ordered Storm	Sample 5	0.3-0.6	60	260	-	-	1800	-	-	0.8
19	O0_200_0.6	Ordered Storm	Sample 5	0.48-0.6	0	200	-	-	1800	-	-	1.2

Notes:

(1): '(J)' denotes jacked installation (instead of suction installation) of the suction bucket in this test.

(2): '(L)' denotes this test was performed with low free fluid height (i.e. ~90 to 100mm above the soil surface) to investigate the water depth (pore fluid cavitation limit) effect.

(3): A range of cyclic frequency was applied in some cyclic loading packets due to the variation of the cyclic load amplitude within the packets.

(4): The summarized displacement rates are for either the standalone monotonic pull-out tests or the post-cyclic monotonic pull-out stages of the cyclic vertical load tests.

(5): The model suction bucket was vented (rather than sealed) during this slow rate monotonic pull-out test to determine the fully drained tensile capacity. This test was also conducted with low free fluid height.

Table 3.4: Mono-Bucket Testing Program

No.	Test ID	Test Nature	Soil Sample	Vertical Stress (kPa)	Horizontal Load								
					Load Frequency (Hz)	Average Cyclic Load[2] (N)	Maximum Cyclic Load Amplitude[2] (N)			Number of Cycles			Displacement Rate for Monotonic Push-over[3] (mm/s)
							Packet 1	Packet 2	Packet 3	Packet 1	Packet 2	Packet 3	
1A	M1_3	Monotonic	Sample 6	120	-	-	-	-	-	-	-	-	3
1B	M1_3r[1]	Monotonic	Sample 8	120	-	-	-	-	-	-	-	-	3
2	M2_0.003	Monotonic	Sample 6	120	-	-	-	-	-	-	-	-	0.003
3A	R45_110_0.6	Random Storm	Sample 7	120	0.6	45 (0.45)	110 (1.1)	220 (2.2)	110 (1.1)	1800	1800	1800	0.8
3B	R45_110_0.6r[1]	Random Storm	Sample 8	120	0.6	45 (0.45)	110 (1.1)	220 (2.2)	110 (1.1)	1800	1800	1800	0.85
4	R90_110_0.6	Random Storm	Sample 7	120	0.6	90 (0.45)	110 (1.1)	220 (2.2)	110 (1.1)	1800	1800	1800	1.1
5	R45_110_0.15	Random Storm	Sample 9	120	0.15	45 (0.45)	110 (1.1)	220 (2.2)	110 (1.1)	1800	1800	1800	0.5
6	R45_110_1.5	Random Storm	Sample 9	120	1.5	45 (0.45)	110 (1.1)	220 (2.2)	110 (1.1)	1800	1800	1800	2.5

Notes:
(1): 'r' denotes this test was a repeat test.
(2): Horizontal load values in bracket are the horizontal load in prototype scale.
(3): The summarized displacement rates are for either the standalone monotonic push-over tests or the post-cyclic monotonic push-over stages of the cyclic horizontal load tests.

Table 3.5: 6 Hours Peak Storm Composition (Andersen, 1991)

Load in % of maximum load	Number of cycles
20	900
37	500
49	200
58	90
64	50
70	30
77	15
83	8
89	4
96	2
100	1
Total number of cycles	**1800**

3.7 Test Data

3.7.1 Multi-bucket Test Data

Factual test data for each multi-bucket test is presented in Appendix A and also provided in separate Microsoft Excel files for each test. Factual test data provided in each Microsoft Excel file is:

- Time in s;
- Vertical stress (vertical load divided by plan area of the model bucket, V/A) in kPa;
- Vertical displacement (z) normalized with bucket skirt length (L), z/L;
- Total pressure measured above bucket lid, TP_A, in kPa;
- Total pressure measured beneath bucket lid, TP_B in kPa; and
- Pore pressure measured beneath bucket lid, PP_B in kPa.

In the multi-bucket tests, positive V/A indicates compression while negative V/A indicates tension. Increase and decrease in vertical displacement (z) of the model multi-bucket indicates penetration and extraction, respectively. Zero vertical displacement value corresponds to the phase when the model bucket skirt tip starts to touch the soil surface.

Through Plate A1 to Plate A23 in Appendix A, the measured vertical stress and excess pore pressure beneath the bucket lid are plotted against bucket vertical displacement normalized by the bucket skirt length (i.e. z/L). In addition, the time history plots for each measurement throughout each test are also presented on the same plates in Appendix A.

Data for each cyclic load packet in each multi-bucket cyclic vertical load test is presented on Plate A24 through to Plate A81 in Appendix A. On these plates, data for cyclic load packet is presented over two plates, as follows:

- The first plate shows (from left to right):

    - Vertical stress (V/A) against normalized vertical displacement (Δz/L, where L is the skirt length and Δz is the change in vertical displacement from the start of the cyclic load packet); and
    - Excess pore pressure and total pressure beneath bucket lid (expressed relative to the hydrostatic pressure, i.e. the measured pore/total pressure deducted by the hydrostatic pressure) against normalized vertical displacement (Δz/L).
- The second plate shows (from top to bottom):
    - The variation of applied vertical stress (V/A) with cycle number (N);
    - The variation of normalized vertical displacement (Δz/L) with cycle number (N); and
    - The variation of excess pore pressure and total pressure beneath bucket lid with cycle number (N).

It should be noted that the presented vertical stress, and any subsequent interpretation of the test data, is based on the measured values rather than the targeted values presented on Plate 8.

3.7.2 Mono-bucket Test Data

Factual test data for each mono-bucket test is presented in Appendix B and also provided in separate Microsoft Excel files for each test. Factual test data provided in each Microsoft Excel file is:

- Time in s;
- Vertical stress (vertical load divided by plan area of the model bucket, V/A) in kPa;
- Vertical displacement (z) normalized with bucket skirt length (L), z/L;
- Horizontal load in prototype scale, $H_{prototype}$, in MN;
- Horizontal displacement at the horizontal loading point (h) normalized with bucket diameter (D), h/D;
- Bucket rotation relative to the vertical axis, θ, in degree;
- Total pressure measured above bucket lid, TP_A, in kPa;
- Total pressure measured beneath bucket lid, TP_B1, TP_B2 and TP_B3, in kPa; and
- Excess pore pressure measured beneath bucket lid, EPP_B1, EPP_B2, in kPa.

In the mono-bucket tests, positive V/A indicates compression, while for the horizontal load, positive values indicate loading toward the leeward side of the OWT. The increase in vertical displacement of the model bucket (z) indicates penetration, with zero vertical displacement corresponding to the phase when the skirt tip starts to touch the soil surface. For the horizontal displacement, positive values indicate displacement toward the leeward side of the bucket from the vertical axis, with positive rotation angle indicating rotation of the bucket towards the leeward side of the OWT from the vertical axis.

Through Plate B1 to Plate B8 in Appendix B, the measured vertical stress and excess pore pressure beneath the bucket lid are plotted against bucket vertical displacement normalized by the bucket skirt length (i.e. z/L); with the measured horizontal load, contact pressure and pore pressure (beneath and above the bucket lid) plotted against horizontal displacement (at

the horizontal loading point) normalized by the bucket diameter (i.e. h/D). In addition, time history plots for each measurement are also presented in Appendix B.

Moment-rotation response measured in each monotonic test is presented on Plate B9 through to Plate B16 in Appendix B, while the data for each cyclic load packet in each mono-bucket cyclic test is presented on Plate 17 through to Plate 46 in Appendix B. On these plates, the data for each cyclic load packet is presented over two plates, as follows:

- The first plate shows:
  - Cyclic moment-rotation response,
  - Variation of moment with cycle number (N),
  - Variation of bucket rotation with cycle number (N).
- The second plate shows:
  - The variation of total pressure beneath bucket lid, $\Delta\sigma_1$, $\Delta\sigma_2$ and $\Delta\sigma_3$ with cycle number (N); and
  - The variation of excess pore pressure beneath bucket lid, Δu_1 and Δu_2 with cycle number (N),

It should be noted that the presented vertical stress and horizontal loads, and any subsequent interpretation of the test data, is based on the measured values rather than the targeted values presented on Plate 10.

4. Discussion on Centrifuge Test Results

4.1 Bucket Installation

Plate 13 and Plate 14 present the resistance to penetration for the multi- and mono-bucket testing, respectively. This is presented in terms of the vertical stress measured during self-penetration and/or jacking in of the bucket, as well as the suction pressure during suction installation. The bucket installation depth generally achieved >95 % of the skirt length, and for tests in which the model bucket could not be fully installed using suction, the foundation was jacked-in (vented) to ensure full touch down.

As shown on Plate 13 and Plate 14, the self-weight penetration resistance profiles for both multi-bucket and mono-bucket tests are generally comparable and within ± 20% of the mean profile, which is consistent with the soil strength variation indicated by CPT profiles (see Plate 6). This suggests that the soil samples used for both multi- and mono-bucket testing were largely consistent.

4.2 Monotonic Load Response

4.2.1 Multi-bucket Test

As discussed previously, the monotonic pull-out tests were conducted either as standalone tests, or after cyclic loading to explore the effect of load history on pull-out capacity. Plate 15 presents all the monotonic vertical pull-out responses (in terms of total vertical stress and excess pore pressure beneath the bucket lid) measured across all tests, and for a range of pull-out rate.

In this section, the observed effects of water depth, installation method and pull-out rate (leading to variable drainage) on the pull-out resistance will be discussed. To facilitate investigation of these effects, Plate 16 features only the responses measured in standalone monotonic pull-out tests. For ease of comparison, the pull-out displacement measured from the "as-installed" position is used (instead of the absolute bucket vertical displacement relative the soil surface) and presented in normalized form as d/L (where d is the pull-out displacement and L is the skirt length).

4.2.1.1 Water Depth Effect

The effect of water depth on suction bucket monotonic pull-out capacity was investigated by conducting fast monotonic pull-out tests (at 3 mm/s) in soil samples with different levels of free fluid above soil surface. Tests M2_3 and M3_3(L) were performed using an identical pull-out rate (i.e. 3 mm/s) but different free fluid height i.e. ~22 m (prototype) in Test M2_3 and ~10 m (prototype) in Test M3_3(L).

As may be expected, reducing the water depth leads to a reduced undrained pull-out capacity. While the stiffness of pull-out response is similar in both tests, up to the vertical

stress of approximately 130 kPa, further displacement leads to Test M2_3 demonstrating a higher pull-out resistance and stiffer response than Test M3_3(L). This deviation in the measured response is believed due to the pore fluid inside the bucket starting to cavitate in Test M3_3(L) when the bucket was pulled beyond the vertical stress of 130 kPa. Given that the only difference between these tests is the height of the free fluid surface, these observations suggest that the pull-out capacity and foundation stiffness of a suction bucket are dependent on the cavitation limit of the pore fluid inside the bucket (per Houlsby et al. 2005b).

4.2.1.2 Installation Method Effect

Tests M1_3(J) and M2_3 were conducted using identical pull-out rate (i.e. 3 mm/s) but with the model bucket installed using two different methods i.e. jacked-in installation in Test M1_3(J) and suction installation in Test M2_3. As shown on Plate 16a, the vertical stress-displacement response measured in both tests (up to -200kPa before Test M1_3(J) was inadvertently halted) is consistent, with both tests reaching a comparable peak resistance. This observation suggests that the suction bucket installation method does not affect the (ultimate) suction bucket monotonic pull-out response.

4.2.1.3 Pull-Out Rate (Drainage) Effect

To investigate the effect of pull-out rate (drainage) on monotonic pull-out response, the maximum pull-out resistance measured in each monotonic pull-out test (standalone or post-cyclic loading) is plotted against pull-out rate on Plate 17.

As shown on Plate 17, the measured maximum pull-out resistance increases with increasing pull-out rate. For the tests conducted with high free fluid height, the maximum pull-out resistance measured at the fastest pull-out rate is more than 10 times greater than the maximum pull-out resistance measured at the slowest (drained) pull-out rate. However, this increase drops to around 7 times greater when tests are performed with lower free fluid height.

Observed increase in pull-out resistance with increasing pull-out rate can be attributed to the high undrained strength of dense to very dense sand (that is higher than its drained strength) and the higher passive suction pressure that can be generated inside the bucket when the bucket is extracted at a faster rate (faster than flow can establish in the soil).

In addition, it can also be observed on Plate 17 that, due to the densification of soil around the suction bucket by cyclic loading, the maximum pull-out resistances measured by the post-cyclic monotonic pull-out tests are generally higher than those measured by the standalone monotonic pull-out tests.

4.2.2 Mono-bucket Test

For the mono-bucket tests, monotonic push-over tests were conducted either as standalone tests or after cyclic horizontal loading to explore the effect of cyclic loading on push-over resistance. Plate 18a and Plate 19 presents all the measured push-over responses (in terms of

overturning moment, excess pore pressure and total contact pressure beneath the bucket lid) as a function of rotation, while Plate 18b shows the overturning moment at a fixed rotation of 5° for a range of push-over rates.

In general, it can be observed on Plate 18a that, regardless of push-over rate, the moment-rotation response is initially stiff, with an apparent 'yield' in the range of 110 to 150 MNm at a rotation of around 0.1° to 0.2°. After reaching this yield point, the moment resistance increases more gradually with further rotation. It can also be noted that the rotation to reach the yield point is approaching the common design criteria for OWTs (i.e. less than 0.5° maximum tilt), which implies that the rotational stiffness of the mono-bucket can be low and may lead to this foundation being unsuitable for OWTs.

In this section, the observed effects of push-over rate (drainage) and the gap between bucket invert and soil on push-over response will be discussed.

4.2.2.1 Push-Over Rate (Drainage) Effect

To investigate the effect of push-over rate (drainage) on mono-bucket response, the monotonic push-over tests (either standalone or post-cyclic loading) were conducted using a range of push over rates (see Table 3.5). Plate 18b summarizes the variation of the measured moment capacity with push-over rate. For the purpose of discussion, the mono-bucket foundation moment capacity is defined as the moment measured at 5° bucket rotation – although similar plots could be generated for lesser rotation.

On Plate 18b, it can be observed that the moment capacity increases with increasing push-over rate. In addition, densification of soil around the model bucket during cyclic loading seems to result in the higher moment resistances observed in the post-cyclic push-over tests as compared to those observed in the standalone monotonic push-over tests. Comparing Plate 18a and Plate 19 indicates that the highest measured negative pore pressure (suction) at the bucket invert corresponds to the highest foundation moment capacity (test R45_110_1.5), while for most tests only modest suction is generated inside the bucket.

For the standalone monotonic push-over tests, the moment capacity measured at the fastest push-over rate is approximately 1.4 times the moment capacity measured at the slowest (drained) push-over rate. This is considerably lower than the rate effect increase observed in the multi-bucket tests (which was greater than 10 times for the tests conducted with high free fluid height, see Plate 17), and is likely reflecting the observations that:

- A bucket foundation without compartmentalization is unable to generate significant differential pore pressure across the width of the bucket invert; and
- Where differential total pressure is generated across the foundation, the lever arm associated with the generated pressure distribution (creating localized push-pull restraint) is modest.

4.2.2.2 Effect of Gap between Bucket Invert and Soil Surface

On Plate 19, it can be observed that the total pressure measured at the σ_1 location (i.e. the leeward edge of the mono-bucket) in tests M1_3 and M2_0.003 did not increase until the model bucket was pushed more than 1° from the vertical axis, indicating that the total stress sensor was not in contact with the soil. In addition, in test M1_3, the pressure readings (excess pore pressure and total pressure) at the u_1, u_2, σ_2 and σ_3 locations appear to increase slightly at the beginning of the test, before decreasing to negative values as rotation increases which also indicate that the bucket invert may not be in full contact with the soil.

Test M1_3 was subsequently repeated as test M1_3r but with a final jacked-in (vented) stage after suction installation, to ensure full touchdown – which was confirmed by an instantaneous increase in $\Delta\sigma_1$ as the moment load was applied to the model bucket (Plate 19). As shown on Plate 18a, despite apparent differences in the touchdown condition, the measured moment-rotation response is remarkably similar. This seems to suggest that a modest gap between the bucket invert and soil surface does not significantly affect the mono-bucket monotonic push-over response.

4.3 Cyclic Load Response

4.3.1 Multi-bucket Test

Cumulative vertical displacements (settlement or uplift) measured in Packet 1 of all the cyclic tests are plotted against cycle number on Plate 20 (for average vertical stress of 60 kPa) and Plate 21 (for average vertical stress of 0 kPa). For cyclic tests with 3 cyclic load packets (as summarized in Table 3.2) the cumulative vertical displacement measured across all 3 packets is plotted against cycle number on Plate 22 through to Plate 27.

As expected, the displacement response of the multi-bucket foundation depends markedly on the cyclic load pattern, cyclic load frequency, average stress and cyclic load amplitude. Detailed interpretation of the data is outside the scope of this project. However, based on the obtained results the effects of cyclic load frequency, cyclic load pattern, cyclic load history and water depth on foundation response will be discussed in the following sections.

4.3.1.1 Cyclic Load Amplitude and Frequency Effect

As is evident from Plate 20, the net displacement under cyclic loading with a compressive average stress is downward (i.e. settlement) despite being cycled into tension up to 200 kPa. However, the response also appears dependent on cyclic load frequency. Some observations of the results presented on Plate 20 are summarized below:

1. As shown by the results for tests R60_160_0.1 and R60_160_0.6, for which the test parameters were identical except for cyclic load frequency, larger settlement was observed in the test conducted with lower frequency. In contrast, the results from testing conducted at higher cyclic load frequency (i.e. test R60_260_1.8 and test R60_260_0.6) indicate that larger settlement observed in the test conducted with higher frequency.

2. Comparisons can also be drawn from tests performed at the same cyclic frequency but with different cyclic load amplitude. Specifically, comparing tests R60_160_0.6 and R60_260_0.6 shows that larger settlement and larger cyclic movements within cycles, observed in test conducted with higher cyclic load amplitude i.e. test R60_260_0.6.

In contrast to above, when the bucket is subjected to 2-way cyclic loading around zero average stress, the foundation tends to be (gradually) pulled out of the soil during the cyclic loading – as shown on Plate 21. Some observations of the results presented on Plate 21 are summarized below:

1. Cyclic load frequency, which reflects drainage condition, impacts the magnitude of displacement. As shown on Plate 21, the vertical displacement observed in test R0_100_0.6 is close to zero despite the bucket being consistently subjected to cyclic tension up to 100 kPa (~3 times the drained pullout capacity of about ~30 kPa, see Plate 16). However, performing the same test at lower cyclic load frequency (test R0_100_0.1) leads to greater upward movement.
2. For tests performed at the same frequency (and with the same storm composition), but with different cyclic load amplitude, the results show that greater uplift occurs for tests experiencing higher cyclic load amplitude. This is evident when comparing test R0_200_0.6 (which applied tension up to 200 kPa, or ~6 times the drained pull-out capacity) with test R0_100_0.6, and also test R0_100_0.1 with test R0_150_0.1.

While it is possible that there are modest differences in bucket embedment between the tests (noting the bucket in all the tests were embedded to >95 % of the skirt length), the results are believed to reliably capture these trends.

In summary, the cyclic tests with random storm patterns confirmed that the bucket vertical displacement (and movement amplitude) is dependent on cyclic load frequency (i.e. drainage condition), as well as both average and cyclic stress levels. Test data seems to support the presence of a 'sweet spot' in term of cyclic load frequency – in this case around 0.6 Hz, with cycling at lower frequency leading to additional settlement or uplift, and cycling at higher frequency leading to higher settlement (due to greater pore pressure generation). These observations suggest that multi-bucket foundations can sustain two-way cyclic loading with significant tension loads (even with zero average stress), and with minimum permanent displacement – provided they are loaded under favorable drainage conditions.

4.3.1.2 Water Depth Effect

Two cyclic tests were conducted to investigate the effect of reduced water depth on the cyclic load performance of multi-bucket foundations. One test was conducted with compressive average stress of 60 kPa (i.e. test R60_260_0.6(L)) which when compared to the same test conducted with higher water depth (i.e. R60_260_0.6), demonstrated much higher displacement within individual large load cycles but smaller overall settlement. A second test was conducted with zero average stress (i.e. test R0_200_0.6(L)), which when compared to the same test conducted with higher water depth (i.e. R0_200_0.6), showed potential for

significant and rapid upward displacement. In summary, these observations confirm the cyclic load performance of multi-bucket foundations is dependent on water depth and the importance of conducting model tests with sufficient water depth to minimize cavitation effects.

4.3.1.3 Cyclic Load Pattern Effect

Multi-bucket vertical displacement response is sensitive to the cyclic vertical load pattern, as evidenced by the test results. As shown on Plate 20, when the bucket is subjected to cyclic vertical load of the same frequency (i.e. tests R60_160_0.6 and U60_160_0.6 or tests R60_160_0.1 and U60_160_0.1), the tests conducted with load pattern comprised repeated cyclic loads with the peak amplitude (i.e. uniform cyclic loading) show higher settlement than that measured in the tests conducted with a random cyclic load pattern. This can be attributed to an increase in the equivalent damage associated with uniform loading, as well as a reduction in the time between large cycles for drainage to occur.

It is also interesting to observe (on Plate 20) the difference in the cyclic load responses caused by ordered and random cyclic loading. Tests R60_260_0.6 and O60_260_0.6 were conducted using the same cyclic load frequency and cyclic vertical load composition, and the results suggest that ordering the load cycles leads to higher accumulated settlement at the end of the test, as well as higher cyclic movement at the time when the largest loads were applied. In addition to the reduced potential for higher accumulated pore pressure (and hence damage) at the time of peak loading, the lower settlement observed in the random storm tests may be attributed to soil densification around the foundation. This (soil densification) is supported by observations of:

1. Higher pull-out resistance measured in post-cyclic monotonic pull-out tests, compared to standalone monotonic pull-out tests (see Plate 17); and
2. Lower vertical displacement measured in the third cyclic load packet of relevant tests, despite the loads mirroring those applied in the first cyclic load packet (see Plate 22 to Plate 27).

Note however that the effect of ordering is less evident in tests performed with zero average load (see Plate 21) and this requires further investigation.

In summary, test observations confirm that the response of multi-buckets to cyclic vertical load response in dense to very dense sands is susceptible to cyclic load pattern. While further work is recommended to understand individual results, the data suggests that uniform and ordered storm load patterns commonly adopted in design may not be appropriate (and may be overly onerous). This is because the beneficial effects of excess pore pressure dissipating between large load cycles are not captured, and the results highlight the need to use cyclic load history generated based on project and site-specific metocean conditions in the design of suction bucket.

4.3.1.4 Cyclic Load History Effect

Results obtained from the cyclic vertical load tests conducted with three cyclic load packets (see Plate 22 to Plate 27) show the beneficial effect of soil densification around the multi-bucket that lead to a 'stiffening' of foundation response over successive packets of cyclic loading. As shown on Plate 22 to Plate 27, smaller bucket displacement was measured in the third cyclic load packet of each test, despite the load frequency and amplitude being identical to the first cycle load packet. These observations highlight a potential optimization opportunity in bucket foundation design if site specific cyclic load history data can be properly defined for a particular site, thereby allowing the benefit of densification from early/ smaller storm load cycles to be accounted for prior to application of the peak design loads.

4.3.2 Mono-bucket Test

Accumulated mono-bucket rotation and vertical displacement (at the center of the foundation) measured in all cyclic horizontal load tests is plotted against cycle number on Plate 28 and Plate 29. Based on these results, the effects of cyclic load frequency, cyclic loading mode and cyclic load history on mono-bucket cyclic load behavior is discussed in the following sections.

It should be noted that the maximum moment applied in any cyclic load package was maintained at a level below the 'yield' moment evident in the monotonic push-over tests. This was selected in order to keep mono-bucket rotation at levels that are (broadly) consistent with typical design constraints, and to explore whether cyclic loading below the initial yield moment would trigger increased rotation.

4.3.2.1 Cyclic Load Frequency Effect

To investigate the effect of cyclic load frequency on the mono-bucket rotation, a series of tests were conducted with the same load regime but at a range of load frequencies, namely tests R45_110_0.6, R45_110_0.6r, R45_110_0.15 and R45_110_1.5 (see Table 3.5).

While the load control for tests conducted at 0.15 Hz and 0.6 Hz (i.e. tests R45_110_0.6, R45_110_0.6r and R45_110_0.15) was achieved well with the achieved loads match target loads, this was not possible for the test conducted at 1.5 Hz (i.e. test R45_110_1.5). In this test, unfortunately, the load control led to a bias in the achieved load with the target loads being achieved in the positive direction but being under achieved in the negative direction. This implies that, in addition to the cyclic load frequency effect, there is some impact from the cyclic loading mode effect (discussed further in Section 4.3.2.2). Accordingly, only the results for tests conducted at the lower frequency are discussed.

As shown on Plate 28 and Plate 29, the accumulated mono-bucket rotation and settlement are higher in the tests conducted at 0.6 Hz (i.e. tests R45_110_0.6, R45_110_0.6r) as compared to the test conducted at 0.15 Hz (i.e. test R45_110_0.15). As shown on Plate 28, the total accumulated bucket rotation measured at the end of tests R45_110_0.6 and R45_110_0.6r is between 0.35 to 0.45 degrees, while the total accumulated bucket rotation measured at the

end of test R45_110_0.15 is less than 0.15 degrees. While not entirely clear, the differences in bucket rotation and settlement observed in the 1st and 2nd cyclic load packet of tests R45_110_0.6 and R45_110_0.6r may be attributed to modest soil variability or differences in installation conditions. Overall, similar to the observations made in the multi-bucket test program, the data suggests that the mono-bucket foundation performance is also dependent on cyclic load frequency (and drainage conditions). In this case, the mono-bucket rotation and settlement increase with modest increases in cyclic loading frequency.

It is also interesting to note the low pore pressure measured at the bucket invert during cyclic loading (as shown on Plate B17 to Plate B46 in Appendix B). Despite relatively large rotations observed in the tests conducted at 0.6 Hz (i.e. tests R45_110_0.6 and R45_110_0.6r), the observed excess pore pressure is small (less than 5 kPa). When combined with the low passive suction pressure observed during the standalone monotonic push-over tests, it may be inferred that significant differential pore pressure cannot be generated across the baseplate in a non-compartmentalized mono-bucket foundation subject to a low net compression load. A non-compartmentalized mono-bucket foundation is therefore an inefficient system in dense to very dense sand for resisting the high moment dominant loading that is applied to an OWT foundation.

4.3.2.2 Cyclic Loading Mode Effect

While all tests were conducted using random storm load sequence, one test (R90_110_0.6 Hz) was performed with higher average load in order to explore the effect of load bias on the mono-bucket cyclic load response. As illustrated on Plate 10, the load regime in this test involved higher positive horizontal loads (but still less than the 'yield' load observed in the standalone monotonic tests) but lower negative horizontal load. Therefore, the applied cyclic loads in this test are more one-way in nature as compared to tests R45_110_0.6 and R45_110_0.6r. Further, as discussed above, the target loads for test R45_110_1.5 could not be fully achieved resulting in a second test (albeit higher frequency) that comprised largely one-way cyclic loading.

In broad terms, it is observed that the moment-rotation response for a mono-bucket foundation is susceptible to the mode of cyclic loading. As shown on Plate 28, the bucket rotation measured in the tests with predominantly one-way cyclic loading (i.e. tests R90_110_0.6 and R45_110_1.5) is smaller than that measured in the tests with high proportion of two-way cyclic loading (i.e. tests R45_110_0.6, R45_110_0.6r), even though the peak positive horizontal load applied in test R90_110_0.6 is the highest among the tests.

4.3.2.3 Cyclic Load History Effect

Similar to the observations in the multi-bucket cyclic tests, the results for the mono-bucket cyclic test also show the beneficial effect of densification around the mono-bucket, leading to a 'stiffening' of foundation response over successive packets of cyclic loading. As shown on Plate 28 and Plate 29, smaller rotation (and negligible settlement) was measured in the third

cyclic load packet of each test, despite the load frequency and amplitude being identical to the first cycle load packet.

5. Laboratory Soil Element Testing

A series of laboratory soil element testing was conducted to characterize the dense to very dense sand used in the multi- and mono-bucket centrifuge tests, in order to facilitate:

1. Detailed interpretation of the centrifuge test results in future (and broader) research projects to support improved understanding of suction bucket foundation response in dense to very dense sand; and
2. Calibration of numerical models and associated design methodologies in future research projects to support design activities for offshore wind farm projects.

Soil element tests were performed on soil sub-sampled from a sample that was prepared and saturated with METHOCEL™ in the same way as the centrifuge soil samples. While challenges exist in recovering 'undisturbed' samples of dense to very dense sand, it is believed that this approach has led to testing on soil samples representative of centrifuge conditions. Note that, except the permeability tests which were conducted with METHOCEL™ as testing fluid, water was used as testing fluid in the simple shear, triaxial, oedometer and bender element tests. However, since the volume of water that entered the soil samples during these tests is small, the use of water in these tests is not expected to significantly affect the METHOCEL™ viscosity and the measured soil responses.

Table 4.1 summarizes all the soil element tests that were carried out for this project. Results for these tests are provided in Appendix C.

Table 5.1: Summary of Soil Element Tests

Test Type	Quantity
Monotonic undrained simple shear (fast rate)	2
Monotonic undrained simple shear (slow rate)	2
Cyclic undrained simple shear	8
Undrained triaxial compression (CAUC)	2
Undrained triaxial extension (CAUE)	2
Drained triaxial compression (CADC)	2
Drained triaxial extension (CADE)	2
Oedometer	2
Permeability	2
Bender element	1
Particle size distribution (PSD)	2

5.1 Particle Size Distribution Test

Two particle size distribution tests were conducted to measure the particle size distribution of the sand used for the centrifuge tests. Measured particle size distributions for the sand

samples are presented in Appendix C and compared to the particle distribution range for the sandy soils at the Massachusetts WEA on Plate 4.

5.2 Simple Shear and Triaxial Tests

Anisotropically consolidated monotonic and cyclic simple shear and monotonic triaxial (compression and extension) tests were conducted to characterize the monotonic and cyclic soil response of the sand used in the multi- and mono-bucket centrifuge tests.

For monotonic simple shear tests, only undrained tests were conducted; while for the monotonic triaxial tests, both undrained and drained tests were conducted. For the undrained cyclic simple shear tests, both one-way and two-way cyclic simple shear tests were conducted. Table 5.2 and Table 5.3 summarize the testing parameters for each simple shear and triaxial tests conducted for this project.

Simple shear and triaxial tests were performed at two vertical consolidation stresses, specifically 60 kPa and 120 kPa. These were selected based on approximate vertical stresses for two representative soil elements in the multi-bucket centrifuge tests:

- Underneath the center of the suction bucket at 6 m below seabed (i.e. half skirt length below the skirt tip), which is shown as position 1 on Figure 5.1. Using an assumed soil submerged unit weight of 10 kN/m^3, the in-situ stress level at this depth is estimated to be 60 kPa. To account for the average vertical stress adopted in most of the cyclic multi-bucket tests (60 kPa in compression) the vertical consolidation stress for this soil element was assumed to be around 120 kPa.
- 6 m below seabed away from the suction bucket, which is shown as position 2 shown on Figure 5.1. The vertical consolidation stress for this soil element was taken as 60 kPa (the estimated in-situ vertical stress).

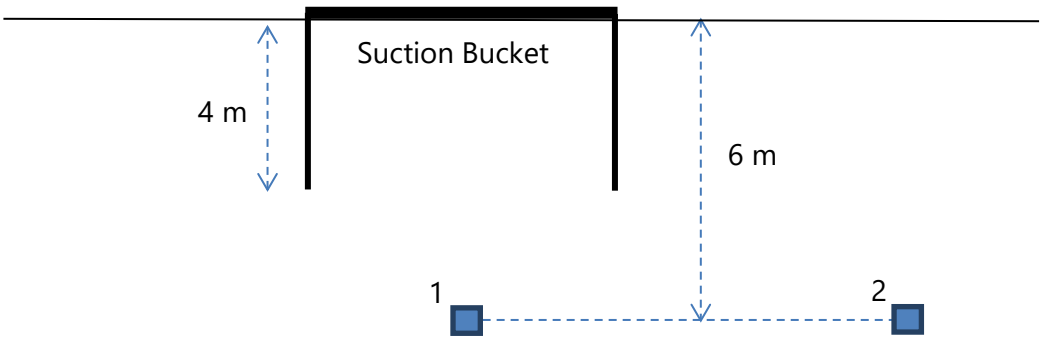

Figure 5.1: Soil Elements Targeted for Simple Shear and Triaxial Tests

To simulate the sequence of (5) ramp up / ramp down cycles applied for each centrifuge samples prior to the bucket testing, all simple shear and triaxial test samples were first consolidated to a vertical stress of 60 kPa (in-situ stress at 6 m below seabed) with K_0 of 0.5 (the red stress path shown on Figure 5.2). Soil samples were then subjected to 5 drained unloading-reloading cycles between vertical stresses of 30 kPa and 60 kPa, while keeping the

lateral stress constant (the blue stress path shown on Figure 5.2). This aims to recreate the estimated total deviatoric stress change (30 kPa) caused by ramping the centrifuge up and down. After this pre-shearing stage, the soil samples were then consolidated at the target consolidation stresses (as summarized in Table 4.2 and Table 4.3). For tests reflecting position 1 shown on Figure 5.1, this follows the green stress path shown on Figure 5.2.

After consolidating at the target final consolidation stresses, a second pre-shearing stage was conducted to mimic the pre-shearing stage adopted in the multi-bucket centrifuge tests, as described below:

- Samples for monotonic triaxial testing were subjected to 400 drained cycles of either ±2 kPa or ± 3 kPa cyclic axial stress depending on the level of vertical consolidation stress. This is shown as the blue stress path shown on Figure 5.3.
- Samples for simple shear testing were subjected to 400 drained cycles of ±1 kPa cyclic shear stress.

All drained pre-shearing was performed at 0.1 Hz. After the second pre-shearing stage, samples were again consolidated under their target consolidation stresses, prior to conducting the specified monotonic or cyclic shearing stage. Measured monotonic and cyclic soil responses are presented in Appendix C.

Table 5.2: Anisotropically Consolidated Simple Shear Testing Program

Test Type	Test Name	Consolidation Stress (kPa)		Monotonic Shear	Cyclic Shear	
		Vertical	Lateral	Rate (%/hr)	Rate (Hz)	Stress (kPa)
Monotonic (slow)	3D-DSS-01	60.0	30.0	5	-	-
Monotonic (fast)	4D-DSS-02	120.0	60.0	5	-	-
Monotonic (slow)	3D-DSS-03	60.0	30.0	2000	-	-
Monotonic (fast)	4D-DSS-04	120.0	60.0	2000	-	-
One-way cyclic	3E-DSS-05	60.0	30.0	-	0.1Hz	0 to 80
One-way cyclic	3E-DSS-06	120.0	60.0	-	0.1Hz	0 to 80
Two-way cyclic	3D-DSS-07	60.0	30.0	-	0.1Hz	-45 to 45
Two-way cyclic	4D-DSS-08	120.0	60.0	-	0.1Hz	-45 to 45
One-way cyclic	2D-DSS-09	60.0	30.0	-	0.1Hz	0 to 150
One-way cyclic	2D-DSS-10	120.0	60.0	-	0.1Hz	0 to 140
Two-way cyclic	2D-DSS-11	60.0	30.0	-	0.1Hz	-100 to 100
Two-way cyclic	3E-DSS-12	120.0	60.0	-	0.1Hz	-90 to 90

Table 5.3: Anisotropically Consolidated Triaxial Testing Program

Test Type	Test Name	Consolidation Stress (kPa)		Monotonic Shear Rate (%/hr)
		Vertical	Lateral	
Undrained Compression	1C-TX-01	60.0	30.0	1
Undrained Compression	2C-TX-02	120.0	60.0	1
Undrained Extension	3C-TX-03	60.0	30.0	1
Undrained Extension	4C-TX-04	120.0	60.0	1
Drained Compression	1B-TX-05	60.0	30.0	0.1
Drained Compression	2B-TX-06	120.0	60.0	0.1
Drained Extension	3B-TX-07	60.0	30.0	1
Drained Extension	4B-TX-08	120.0	60.0	0.1

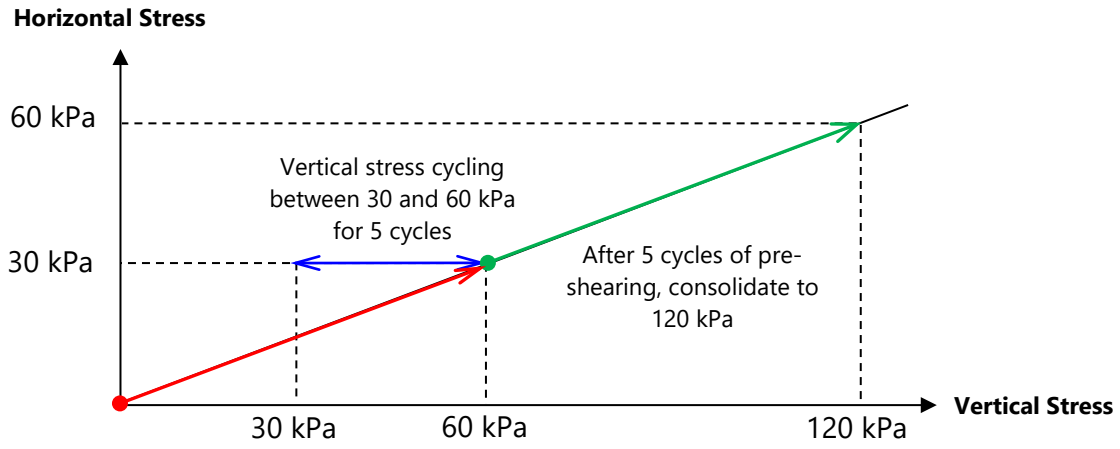

Figure 5.2: Stress path for pre-shearing stage 1

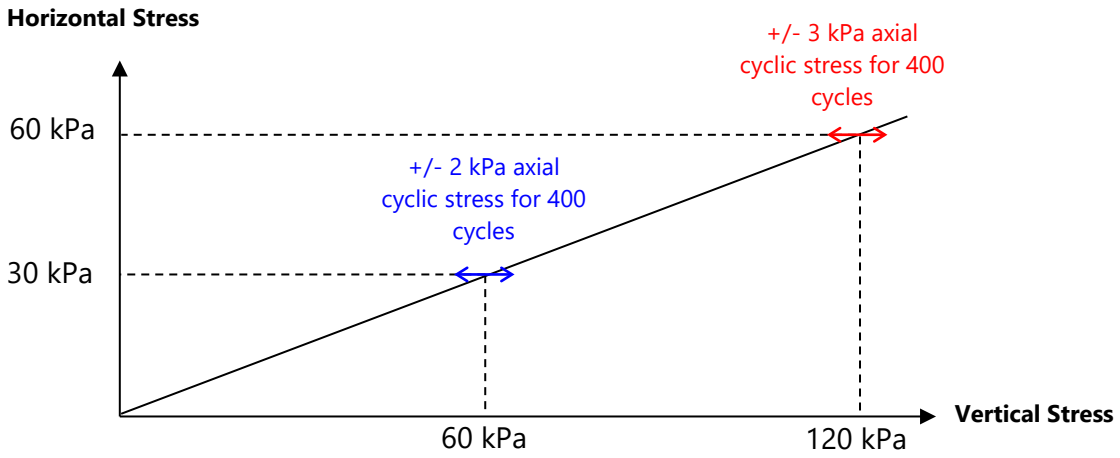

Figure 5.3: Stress path for second pre-shearing stage of triaxial tests

5.3 Oedometer Tests

Two oedometer tests were conducted to characterize the compressibility and consolidation characteristics of the sand samples used in the multi-bucket and mono-bucket centrifuge tests. Oedometer tests conducted using the load steps are summarized in Table 5.4, and the results are presented in Appendix C.

Table 5.4: Load Steps in Oedometer Tests

Load Step	Vertical Stress (kPa)
1	10
2	20
3	40
4	80
5	40
6	20
7	40
8	80
9	160
10	320
11	640
12	1280
13	10

5.4 Permeability Test

Two constant head permeability tests were conducted to measure the coefficient of permeability for the sand samples used in the centrifuge tests. METHOCEL™ fluid that was used to saturate the soil samples was used as testing fluid in these permeability tests. Measured coefficient of permeability for the sand samples (saturated with METHOCEL™) is presented in Appendix C.

5.5 Bender Element Test

A series of bender element tests was conducted to measure small strain shear modulus (G_0) at different effective stress levels and loading histories (i.e. at different overconsolidation ratios).

The test was performed in 9-stages, with the sample consolidated isotropically in a triaxial cell following the consolidation mean stress sequence of 20, 40, 80, 40, 20, 40, 80, 160 and 320 kPa. During consolidation, the sample height and volume change were measured to calculate changes in specimen height and density.

Bender element tests were performed at the end of each consolidation stage. A shear wave was triggered at one end of the sample via the piezo-ceramic element (the transmitter) using

a function generator. Input frequency was varied in order to generate a clear signal, which then propagated along the length of the sample and was detected on arrival by a second piezo-ceramic element (the receiver) located at the other end of the sample. Signals were recorded and processed to determine the travel time (Δt). The G_0 was then calculated using the determined Δt, current sample height and density.

Measured small strain shear modulus (G_0) at various effective stress levels and loading history are presented in Appendix C.

6. Conclusions and Recommendations for Future Work

6.1 Conclusions

The ultimate objective of this project was to generate data from high quality and well documented experimental testing of bucket foundations in soil conditions relevant to offshore wind farm developments off the U.S. East Coast, in order to facilitate future improvements in the design methods for such foundations. To achieve this, a large number of centrifuge tests (23 multi-bucket tests and 8 mono-bucket tests, in 9 soil samples) have been conducted as well as an extensive program of soil element tests on the sand used in the centrifuge tests. Key advantages of the current dataset as compared to other datasets available in the public domain are:

1. Cyclic load patterns that were adopted in the centrifuge tests are more realistic and mimic the real random storm load pattern. The majority of the published experimental studies (e.g. Kelly et al., 2006; Bienen et al., 2018) on suction buckets examined packets of uniform or ordered cyclic loading.
2. Water cavitation was recognized as a critical issue in controlling the uplift response and hence much larger (and more realistic) water depths were modelled in these tests than in other public domain datasets.
3. Centrifuge tests were supplemented by a series of companion soil element tests that characterized the behavior of the tested sand. This is expected to facilitate back analysis and numerical simulation as part of future (and broader) research.
4. The dataset will allow direct comparison between the performance and efficiency of mono- and multi-bucket foundation configurations in the same soil.

Based on the obtained multi-bucket and mono-bucket test results, as discussed in Section 4, the main observations of the test results are summarized below:

1. Monotonic Load Response

a. The suction bucket pull-out capacity and stiffness are dependent on the water depth (where the suction bucket will be installed) which dictates the cavitation limit of pore fluid inside the bucket.
b. The suction bucket pull-out capacity in dense to very dense sand increases with increasing pull-out rate and will be ultimately limited by the pore fluid cavitation limit and the undrained pull-out capacity, whichever is smaller.
c. Limited test results seem to suggest that the suction bucket installation method (jacked-in or suction installation) does not significantly affect the suction bucket monotonic pull-out response.
d. The mono-bucket foundation moment capacity increases with increasing push-over rate but the effect of push-over rate on the moment capacity seems significantly smaller than the effect of pull-out rate on the pull-out capacity for the multi-bucket system.

e. Limited test results appear to suggest that the presence of a small gap between the bucket invert and soil surface may not significantly affect the monotonic push-over response and moment capacity for a non-compartmentalized mono-bucket.
f. Due to densification of soil around the model bucket during cyclic loading, both pull-out capacity and moment capacity measured in post-cyclic monotonic tests are higher than measured in standalone monotonic tests.

2. Cyclic Load Response

a. Results of the cyclic vertical load test (multi-bucket system) confirm that the suction bucket vertical displacement and stiffness response when subject to cyclic tensile loading are highly dependent on the cyclic load frequency (i.e. drainage condition), as well as both average and cyclic load levels. Data suggests that under identical cyclic amplitudes, the permanent displacement (either settlement or uplift) may be largest when the suction bucket is subjected to either a low (quasi-drained) or high (quasi-undrained) cyclic load frequency. Consequently, the most favorable cyclic frequency for suction buckets in sand under long-term cyclic loading occurs for intermediate loading conditions (i.e. where partially drained/ undrained conditions occur during a single cycle but where rapid drainage times ensure minimal accumulation of excess pore pressure from cycle to cycle). Data also reflected that under favorable drainage conditions and with a sufficiently high cavitation pressure limit, the suction bucket is potentially able to sustain two-way cyclic loading with significant tension loads at close to zero average load, with minimal permanent displacement.
b. Results of the cyclic vertical load tests (multi-bucket system) conducted with various cyclic load patterns indicate greater vertical accumulated displacement in tests conducted with uniform and ordered storm load patterns as compared to randomized distributions of cyclic load. These results therefore suggest that assuming uniform or ordered storm load patterns is excessively onerous for design of suction bucket foundations in dense to very dense sand. This is because the beneficial dissipation of excess pore pressure between the initial large load cycles (which densifies the soil around the bucket and reduces degradation of the undrained strength and stiffness caused by cyclic loading) occurs to a lesser degree in the experimental simulation when using the simplified (i.e. ordered or uniform) cyclic load patterns. These test results highlight the importance of site-specific cyclic load history data for optimal design of suction bucket foundations in dense to very dense sand.
c. Results of the cyclic horizontal test results (mono-bucket system) indicate that the rotational stiffness of a mono-bucket foundation is affected by the cyclic load frequency with the accumulated bucket rotation and vertical settlement increasing with increasing cyclic loading frequency. In addition, it was also observed that the pore pressure and total pressure changes at the bucket invert during cyclic loading was generally small and the maximum suction pressure measured at the bucket

invert in the fastest standalone monotonic push-over tests was also generally small when compared to the pore fluid cavitation limits. This suggests that significant differential pore pressure cannot be generated across the baseplate in a non-compartmentalized mono-bucket foundation subject to a low net compression load. A non-compartmentalized mono-bucket foundation is therefore an inefficient system in dense to very dense sand for resisting the high moment dominant loading that is applied to an OWT foundation.

d. Cyclic horizontal load test results (mono-bucket system) suggest that the moment-rotation response for a mono-bucket foundation system is influenced by the mode of cyclic loading. Specifically, the observed bucket rotation was significantly smaller when the mono-bucket was subject to one-way cyclic loading as compared to when it was subject to two-way cyclic loading.
e. In both multi- and mono-bucket tests, due to densification of soil around the suction buckets following dissipation of excess pore pressures generated by the first two cyclic load packets, the bucket displacement or rotation measured in the 3rd cyclic load packet were generally smaller than those measured in the 1st cycle load packets for the same test, even though both cyclic load packets were identical. These observations highlight a potential optimization opportunity in bucket foundation design if site specific cyclic load history data can be properly defined for a particular site, thereby allowing the benefit of densification from early/ smaller storm load cycles to be accounted for prior to application of the peak design loads.

In summary, the centrifuge test data collected for this project suggests that, as compared to the mono-bucket system, the multi-bucket system is a more efficient foundation system in resisting the high overturning moment loading for OWTs in dense to very dense sand. This is because passive suction is easier to be generated by the "push-pull" effect between the windward bucket and leeward bucket of the multi-bucket system, as compared to the rotational mechanism of the mono-bucket system. In addition, the individual buckets in a multi-bucket foundation system can be widely separated allowing for much more efficient transmission of the applied overturning moment into the soil compared with a mono-bucket system. Hence to achieve the same total foundation capacity the amount of steel required to fabricate a mono-bucket system will be much greater than for an equivalent multi-bucket system. However, this might be offset to some degree by the additional framing required to join the multi-bucket system together.

In addition, the test data showed that under favorable drainage conditions (the 'sweet spot') and with a sufficiently high cavitation pressure limit, the suction buckets of a multi-bucket foundation system can sustain two-way cyclic loading with significant tension loads at close to zero average stress, with minimal permanent displacement. This could eliminate any perceived requirement for expensive foundation ballast to offset the applied cyclic tension loads.

It is anticipated that with further research using the data collected for this project, the multi-bucket foundation system will be proven to be a technically viable (and hopefully economical) foundation option to support offshore wind turbines located of the U.S. East Coast in seabeds comprised of dense to very dense sand.

6.2 Recommendations for Future Work

Due to the superior efficiency of a "multi-bucket" foundation system in resisting the high overturning moment loads applied to OWT foundations, the following future work is recommended in order to focus development of an improved design methodology for optimal design of cost-effective "multi-bucket" foundation system for OWTs in dense to very dense sand.

6.2.1 Numerical Analysis

The comprehensive centrifuge test and soil element test dataset collected for this project has offered an excellent opportunity for the development and implementation of appropriate effective stress constitutive soil models and numerical modelling techniques that can best predict the key soil behaviors pertinent to the design of suction buckets subject to cyclic tensile loading in dense to very dense sand. Such soil behaviors include appropriate contractive/ dilative characteristics of sand and explicit consideration of the effects of pore fluid cavitation on the soil and foundation response.

Advanced effective stress constitutive soil models are preferred since these could realistically simulate (i) high undrained/ partially drained tension capacity during transient tension loading, and (ii) pore water dissipation between large load cycles that densify the soil around the bucket and eliminate ongoing degradation of the undrained strength and stiffness from load cycle to load cycle.

Soil element test data collected during this project can be used to parameterize an appropriate effective stress constitutive soil model implemented within a suitable numerical analysis package. With the parameterized soil model, numerical analysis could be conducted to predict the response of the suction bucket monotonic and cyclic load tests conducted for this project. Predicted monotonic and cyclic responses (and hence the soil model and numerical modelling technique) can be validated from these test data.

Armed with a validated constitutive soil model and numerical modelling technique, parametric studies are recommended to identify key factors that govern the cyclic tension capacity of suction bucket in sand which could in turn contribute to the development of a robust framework for the design of cost-effective suction bucket foundation for OWTs in sand.

6.2.2 Centrifuge Tests with Realistic Storm Load History

Cyclic vertical load tests have shown that the suction bucket vertical displacement and stiffness response under cyclic vertical loading are highly dependent on the cyclic load

frequency (i.e. drainage condition) and cyclic load pattern, as well as both average and cyclic stress levels. In this project, the storm cyclic load patterns (random or ordered) adopted in the centrifuge tests were generated artificially from the 6-hour duration peak storm load composition outlined in Andersen (1991).

It is recommended that an additional set of centrifuge tests be conducted using site specific storm load time history data, most representative of actual conditions that will be encountered at an offshore U.S. site. Ideally such a dataset could comprise a measured storm load history, or in lieu of such data, could comprise a synthetic storm load history derived from site specific metocean data applied to an example prototype structure.

This new dataset could be used to further validate the analysis approach developed as per Section 6.2.1 and confirm (or otherwise) the appropriateness of idealized and simplified storm load histories, such as outlined in Andersen (1991) and used as the basis for the tests presented in this report.

7. References

Andersen, K.H., (1991). Foundation design of offshore gravity structures. in 'Cyclic Loading of Soils', Blackie, London, 122-173.

Andersen, K.H., (2015). Cyclic soil parameters for offshore foundation design. The Third ISSMGE McClelland lecture. In Frontiers in offshore geotechnics III (ISFOG) (ed. V. Meyer), pp. 5–82. Boca Raton, FL, USA: CRC Press (Taylor & Francis).

Bienen, B., Klinkvort, R. T., O'Loughlin, C. D., Zhu, F. Y., and Byrne, B. W. (2018) Suction caissons in dense sand, Part II: Vertical cyclic loading into tension. Géotechnique, 68, No. 11, 953-967.

Bye, A, Erbrich, CT, Rognlien, B, and Tjelta, TI. (1995). Geotechnical experience from the installation of the Europipe jacket with bucket foundations. Proc., Offshore Technology Conf., OTC 7795, 27th Ed., 897–908.

Chow S.H., Roy, A., Herduin, M., Heins, E., King, L., Bienen, B., O'Loughlin, C., Gaudin, C., and Cassidy, M. (2018). Characterisation of UWA superfine silica sand. Oceans Graduate School, Release: 18844.

De Catania S., Breen J., Gaudin C. and White D.J. (2010). Development of multiple-axis actuator control system. Int. Conf. on Physical Modelling in Geotechnics. Zurich, Switzerland, 325-330.

Fugro (2016). Effects of Cyclic Loading on Suction Bucket Foundations for Offshore Wind Turbines, Report prepared for the Bureau of Safety & Environmental Enforcement (BSEE), Fugro Consultants, Inc. Project No. 04.76160003.

Gaudin C., White D.J., Boylan N. Breen J., Brown T.A., De Catania S., and Hortin P. (2009). A wireless data acquisition system for centrifuge model testing. Measurement Science and Technology. 20, No 095709.

Houlsby, G. T., Kelly, R. B. and Byrne, B. W. (2005). The tensile capacity of suction caissons in sand under rapid loading. Frontiers in Offshore Geotechnics: ISFOG 2005 – Gourvenec & Cassidy (eds), Taylor & Francis Group, 405-410.

House, A. R. (2002) Suction caisson foundations for buoyant offshore facilities. PhD thesis, The University of Western Australia, Perth, Australia.

Kelly, R. B., Houlsby, G. T. and Byrne, B. W. (2006). Transient vertical loading of model suction caissons in a pressure chamber. Géotechnique, 56, No. 10, 665–675.

Randolph, M.F., Jewell, R.J., Stone, K.J.L. and Brown, T.A. (1991). Establishing a new centrifuge facility. Proc. Centrifuge 1991 (eds H.-Y. Ko and F. G. McLean), pp. 2–9. Rotterdam, the Netherlands: A.A. Balkema.

Tjelta, TI. (2015). The suction foundation technology. In: Meyer V (ed.). Proc. Int. Symp. Frontiers in Offshore Geotechnics, ISFOG III. London: Taylor and Francis, 85–93.

List of Plates

Plate 1: UWA Beam Centrifuge

Plate 2: Experimental Arrangement of Multi-bucket testing

Plate 3: Experimental Arrangement of Mono-bucket testing

Plate 4: Particle Size Distribution Range for Sands at One of the OWF Sites in the Massachusetts Area

Plate 5: Test Layout for Multi-Bucket and Mono-Bucket Tests

Plate 6: CPT Profiles Measured in Centrifuge Soil Samples Used for Multi-Bucket and Mono-Bucket Tests

Plate 7: Definition of Loads in Mono-Bucket Test

Plate 8: Cyclic Load Packets (Multi-Bucket Test)

Plate 9: Relationships between Cyclic Load Frequency and Cyclic Load Amplitude

Plate 10: Cyclic Load Packets (Mono-Bucket Test)

Plate 11: Centrifuge Testing Sequence (Multi-Bucket Test)

Plate 12: Centrifuge Testing Sequence (Mono-Bucket Test)

Plate 13: Installation Responses (Multi-Bucket Test)

Plate 14: Installation Responses (Mono-Bucket Test)

Plate 15: Monotonic and Post-cyclic Monotonic Pull-out Responses (Multi-Bucket Tests)

Plate 16: Monotonic Pull-out Responses (Multi-Bucket Test)

Plate 17: Variation of Maximum Pull-out Resistance with Pull-out Rate (Multi-Bucket Test)

Plate 18: Moment-rotation Responses during Monotonic and Post-cyclic Monotonic Push-over (Mono-bucket Test)

Plate 19: Pressure-rotation Responses during Monotonic and Post-cyclic Monotonic Push-over (Mono-bucket Test)

Plate 20: Comparison of Displacement for Multi-bucket Tests with Average Vertical Stress of 60 kPa (Packet 1)

Plate 21: Comparison of Displacement for Multi-bucket Tests with Average Vertical Stress of 0 kPa (Packet 1)

Plate 22: Comparison of Displacement for Cyclic Load Packets 1, 2 and 3 (Test R60_160_0.1)

Plate 23: Comparison of Displacement for Cyclic Load Packets 1, 2 and 3 (Test R60_160_0.6)

Plate 24: Comparison of Displacement for Cyclic Load Packets 1, 2 and 3 (Test R0_100_0.1)

Plate 25: Comparison of Displacement for Cyclic Load Packets 1, 2 and 3 (Test R0_100_0.6)

Plate 26: Comparison of Displacement for Cyclic Load Packets 1, 2 and 3 (Test U60_160_0.1)

Plate 27: Comparison of Displacement for Cyclic Load Packets 1, 2 and 3 (Test U60_160_0.6)

Plate 28: Variation of Bucket Rotation with Cycle Number (Mono-bucket Test)

Plate 29: Variation of Vertical Disp. with Cycle Number (Mono-bucket Test)

Appendix A

Multi-Bucket Test Data

Appendix B

Mono-Bucket Test Data

Appendix C

Soil Element Test Data